Human tribbles, a protein family controlling mitogen-activated protein kinase cascades. *J. Biol. Chem.* 279:42703–42708.
9. Wilkin, F., N. Suarez-Huerta, B. Robaye, J. Peetermans, F. Libert, J.E. Dumont, and C. Maenhaut. 1997. Characterization of a phosphoprotein whose mRNA is regulated by the mitogenic pathways in dog thyroid cells *Eur. Eur. J. Biochem.* 248:660–668.
10. Mayumi-Matsuda, K., S. Kojima, H. Suzuki, and T. Sakata. 1999. Identification of a novel kinase-like gene induced during neuronal cell death. *Biochem. Biophys. Res. Commun.* 258:260–264.
11. Wu, M., L.G. Xu, Z. Zhai, and H.B. Shu. 2003. SINK is a p65-interacting negative regulator of NF-κB-dependent transcription. *J. Biol. Chem.* 278:27072–27079.
12. Kiss-Toth, E., D.H. Wyllie, K. Holland, L. Marsden, V. Jozsa, K.M. Oxley, T. Polgar, E.E. Qwarnstrom, and S.K. Dower. 2006. Functional mapping and identification of novel regulators for the Toll/Interleukin-1 signalling network by transcription expression cloning. *Cell. Signal.* 18:202–214.
13. Uematsu, S., M. Matsumoto, K. Takeda, and S. Akira. 2002. Lipopolysaccharide-dependent prostaglandin E(2) production is regulated by the glutathione-dependent prostaglandin E(2) synthase gene induced by the Toll-like receptor 4/MyD88/NF-IL6 pathway. *J. Immunol.* 168:5811–5816.
14. Gorgoni, B., D. Maritano, P. Marthyn, M. Righi, and V. Poli. 2002. C/EBPβ gene inactivation causes both impaired and enhanced gene expression and inverse regulation of IL-12 p40 and p35 mRNAs in macrophages. *J. Immunol.* 168:4055–4062.
15. Ramji, D.P., and P. Foka. 2002. CCAAT/enhancer-binding proteins: structure, function and regulation. *Biochem. J.* 365:561–575.
16. Plevy, S.E., J.H. Gemberling, S. Hsu, A.J. Dorner, and S.T. Smale. 1997. Multiple control elements mediate activation of the murine and human interleukin 12 p40 promoters: evidence of functional synergy between C/EBP and Rel proteins. *Mol. Cell. Biol.* 17:4572–4588.
17. Zhu, C., K. Gagnidze, J.H. Gemberling, and S.E. Plevy. 2001. Characterization of an activation protein-1-binding site in the murine interleukin-12 p40 promoter. Demonstration of novel functional elements by a reductionist approach. *J. Biol. Chem.* 276:18519–18528.
18. Bradley, M.N., L. Zhou, and S.T. Smale. 2003. C/EBPβ regulation in lipopolysaccharide-stimulated macrophages. *Mol. Cell. Biol.* 23:4841–4858.
19. Seher, T.C., and M. Leptin. 2000. Tribbles, a cell-cycle brake that coordinates proliferation and morphogenesis during *Drosophila* gastrulation. *Curr. Biol.* 10:623–629.
20. Mata, J., S. Curado, A. Ephrussi, and P. Rorth. 2000. Tribbles coordinates mitosis and morphogenesis in *Drosophila* by regulating string/CDC25 proteolysis. *Cell.* 101:511–522.
21. Grosshans, J., and E. Wieschaus. 2000. A genetic link between morphogenesis and cell division during formation of the ventral furrow in *Drosophila*. *Cell.* 101:523–531.
22. Rorth, P., K. Szabo, and G. Texido. 2000. The level of C/EBP protein is critical for cell migration during *Drosophila* oogenesis and is tightly controlled by regulated degradation. *Mol. Cell.* 6:23–30.
23. Keeshan, K., Y. He, B.J. Wouters, O. Shestova, L. Xu, H. Sai, C.G. Rodriguez, I. Maillard, J.W. Tobias, P. Valk, et al. 2006. Tribbles homolog 2 inactivates C/EBPα and causes acute myelogenous leukemia. *Cancer Cell.* 10:401–411.
24. Ohoka, N., S. Yoshii, T. Hattori, K. Onozaki, and H. Hayashi. 2005. TRB3, a novel ER stress-inducible gene, is induced via ATF4-CHOP pathway and is involved in cell death. *EMBO J.* 24:1243–1255.
25. Du, K., S. Herzig, R.N. Kulkarni, and M. Montminy. 2003. TRB3: a tribbles homolog that inhibits Akt/PKB activation by insulin in liver. *Science.* 300:1574–1577.
26. Koo, S.H., H. Satoh, S. Herzig, C.H. Lee, S. Hedrick, R. Kulkarni, R.M. Evans, J. Olefsky, and M. Montminy. 2004. PGC-1 promotes insulin resistance in liver through PPAR-alpha-dependent induction of TRB-3. *Nat. Med.* 10:530–534.
27. Qi, L., J.E. Heredia, J.Y. Altarejos, R. Screaton, N. Goebel, S. Niessen, I.X. Macleod, C.W. Liew, R.N. Kulkarni, J. Bain, et al. 2006. TRB3 links the E3 ubiquitin ligase COP1 to lipid metabolism. *Science.* 312:1763–1766.
28. Yamamoto, M., T. Okamoto, K. Takeda, S. Sato, H. Sanjo, S. Uematsu, T. Saitoh, N. Yamamoto, H. Sakurai, K.J. Ishii, et al. 2006. Key function for the Ubc13 E2 ubiquitin-conjugating enzyme in immune receptor signaling. *Nat. Immunol.* 7:962–970.
29. Tanaka, T., S. Akira, K. Yoshida, M. Umemoto, Y. Yoneda, N. Shirafuji, H. Fujiwara, S. Suematsu, N. Yoshida, and T. Kishimoto. 1995. Targeted disruption of the NF-IL6 gene discloses its essential role in bacteria killing and tumor cytotoxicity by macrophages. *Cell.* 80:353–361.
30. Shen, F., Z. Hu, J. Goswami, and S.L. Gaffen. 2006. Identification of common transcriptional regulatory elements in interleukin-17 target genes. *J. Biol. Chem.* 281:24138–24148.

Signal Transducer and Activator of Transcription 3 Signaling Within Hepatocytes Attenuates Systemic Inflammatory Response and Lethality in Septic Mice

Ryotaro Sakamori,[1]* Tetsuo Takehara,[1]* Chihiro Ohnishi,[1] Tomohide Tatsumi,[1] Kazuyoshi Ohkawa,[1] Kiyoshi Takeda,[2] Shizuo Akira,[3] and Norio Hayashi[1]

Sepsis is an infection-induced syndrome with systemic inflammatory response leading to multiorgan failure and occasionally death. During this process, signal transducer and activator of transcription 3 (STAT3) is activated in the liver, but the significance of this molecule has not been established. We generated hepatocyte-specific STAT3-deficient mice (L-STAT3 KO) and examined the susceptibility of these mice to cecal ligation and puncture–induced peritonitis, a well-established septic model. L-STAT3 KO mice showed significantly higher mortality and produced lesser amounts of various acute phase proteins than control littermates. Although blood bacterial infection did not differ between L-STAT3 KO mice and control mice, the former showed deterioration of the systemic inflammatory response as evidenced by a significant increase in various cytokines such as tumor necrosis factor α, IFN-γ, IL-6, IL-10, monocyte chemoattractant protein 1, and macrophage inflammatory protein 1β. A similar hyperinflammatory response was observed in another septic model caused by lipopolysaccharide (LPS) injection. In vitro analysis revealed that soluble substances derived from hepatocytes and dependent on STAT3 were critical for suppression of cytokine production from LPS-stimulated macrophage and splenocytes. *Conclusion:* STAT3 activation in hepatocytes can attenuate a systemic hyperinflammatory response and lethality in sepsis, in part by suppressing immune cell overactivation, implying a critical role of hepatocyte STAT3 signaling in maintaining host homeostasis. (HEPATOLOGY 2007;46: 1564-1573.)

Signal transducer and activator of transcription 3 (STAT3) mediates a signal from the IL-6 family of cytokines such as IL-6, oncostatin M, leukemia inhibitory factor, and ciliary neutrophic factor, and activates transcription of various target genes.[1] Although a STAT3 is now known to be ubiquitously expressed in variety of cells and has pleiotropic functions, it was formerly termed *acute phase response factor* and was first identified in the liver as an inducible DNA binding protein binding to type 2 IL-6–responsive elements within the promoter of hepatic acute phase protein (APP) genes.[2,3] Because deletion of STAT3 leads to embryonic lethality in mice, the significance of STAT3 in adult organs has been investigated using conditional knockout animals generated by the Cre/loxP recombination system.[4] Research has shown that STAT3 signaling within hepatocytes controls a variety of physiological or pathological processes, including hepatocyte proliferation after partial hepatectomy,[5] apoptosis resistance of hepatocytes during Fas-mediated liver injury,[6] and regulation of hepatic gluconeogenic genes.[7] Although STAT3 is activated in response to a rise of circulating cytokines, the significance of hepatic STAT3 has not been elucidated under systemic inflammatory conditions.

Sepsis is an infection-induced systemic syndrome, the incidence of which is estimated at 750,000 cases annually in North America with overall mortality being approxi-

Abbreviations: APP, acute phase protein; CLP, cecal ligation and puncture; LPS, lipopolysaccharide; L-STAT3 KO, hepatocyte-specific STAT3-deficient mice; STAT3, signal transducer and activator of transcription 3; TNF-α, tumor necrosis factor α; TUNEL, terminal deoxynucleotidyl transferase-mediated dUTP nick end-labeling.

From the [1]Department of Gastroenterology and Hepatology, Osaka University Graduate School of Medicine, Osaka, Japan; the [2]Department of Molecular Genetics, Medical Institute of Bioregulation, Faculty of Medical Sciences, Kyushu University, Fukuoka, Japan; and the [3]Department of Host Defense, Research Institute for Microbial Diseases, Osaka University, Osaka, Japan.

Received March 13, 2007; accepted May 25, 2007.

Supported by a grant-in-aid for Scientific Research from the Ministry of Education, Culture, Sports, Science, and Technology, Japan.

*These authors contributed equally to this study.

Address reprint requests to: Dr. Norio Hayashi, Department of Gastroenterology and Hepatology, Osaka University Graduate School of Medicine, 2-2 Yamada-oka, Suita, Osaka 565-0871, Japan. E-mail: hayashin@gh.med.osaka-u.ac.jp; fax: (81)-6-6879-3629.

Published online in Wiley InterScience (www.interscience.wiley.com).

DOI 10.1002/hep.21837

Potential conflict of interest: Nothing to report.

Supplementary material for this article can be found on the HEPATOLOGY website (http://interscience.wiley.com/jpages/0270-9139/suppmat/index.html).

mately 30%, but rising to 40% in the elderly.[8] Sepsis develops when the initial, appropriate host response to an infection becomes amplified and then dysregulated.[9] Among those harmful or damaging responses is the rise of a variety of circulating cytokines such as IL-6, tumor necrosis factor α (TNF-α), IL-10, and IFN-γ. These cytokines lead directly to the development of systemic inflammatory response syndrome. During this process, an increasing proportion of patients will develop adult respiratory distress syndrome, disseminated intravascular coagulation, and/or acute renal failure, leading to the multiple organ dysfunction syndrome.[10] The liver is also one of the target organs of multiple organ dysfunction syndrome, although liver dysfunction may cause patient death less frequently than cardiovascular dysfunction.[11] Conversely, sepsis is a serious complication of severe liver diseases such as fulminant hepatitis[12] and decompensated cirrhosis.[13] Thus, research on the relevance of signal transduction in liver cells in the septic condition would not only satisfy basic scientific interest but would also have clinical implications.

In the present study, we used hepatocyte-specific STAT3-deficient (L-STAT3 KO) mice and examined the significance of STAT3 signaling within hepatocytes in a well-established murine model of sepsis. We found that STAT3 deficiency in hepatocytes causes exacerbation of the hyperinflammatory response by attenuating hepatic production of soluble substances that can suppress immune cell activation and also increases mortality in septic mice. This study identified an anti-inflammatory function of hepatic STAT3 signaling and its protective role against systemic inflammation, providing genetic evidence for a close link between hepatocytes and the immune system.

Materials and Methods

Animals. Mice carrying a STAT3 gene with 2 *loxP* sequences flanking exon 22 and a STAT3 null allele (*STAT3 fl/−*) have been described previously.[14] To generate mice with hepatocyte-specific STAT3 deficiency, we crossed STAT3 fl/− mice and Alb-Cre transgenic mice,[15] which express the Cre recombinase gene under the regulation of the albumin gene promoter. We crossed Alb-Cre STAT3 fl/fl mice and STAT3 fl/− mice. The resulting Alb-Cre STAT3 fl/− mice were used as L-STAT3 KO mice. Sex-matched STAT3 fl/− mice obtained from the same litter were used as control mice. All mice were used at the age of 12-15 weeks. All animals were housed under specific pathogen-free conditions and were treated with humane care under approval from the Animal Care and Use Committee of Osaka University Medical School.

Cecal Ligation and Puncture and Lipopolysaccharide Injection. Cecal ligation and puncture (CLP) is a well-established murine model of septic shock. The mice underwent CLP surgery as described previously.[16] In brief, the mice were anesthetized via intraperitoneal injection of sodium pentobarbital. Under sterile condition, the cecum was assessed via a 1-cm midline incision of the lower abdomen, ligated with a suture below the ileocecal valve, and punctured once with a 23-gauge needle. The cecum was replaced in the peritoneum, and the abdomen was closed with sutures. The mice were injected with 1 mL of lactate Ringer's solution subcutaneously for fluid resuscitation. As another septic model, lipopolysaccharide (LPS) (form *Escherichia coli* 055: B5; Sigma, St. Louis, MO) was injected intraperitoneally at a dose of 4 mg/kg body weight.

Preparation of Peritoneal Macrophage. To isolate peritoneal macrophages, we injected mice intraperitoneally with 2 mL of 4% thioglycollate. Peritoneal exudates cells were isolated from the peritoneal cavity 4 days after injection. The cells were incubated for 4 hours in 96-well plates and washed 3 times with phosphate-buffered saline. We used the adherent cells as peritoneal macrophages for further experiments.

Determination of the Bacterial Load. Mice were sacrificed 24 hours after CLP surgery. Samples of blood were obtained in sterile condition. Fifty microliters of the blood were then plated on heart-infusion plates. The heart-infusion plates were incubated at 37°C overnight, and the number of bacteria colonies was counted. Results were expressed as $\log_{10}$ of CFU.

Blood Biochemistry. Blood samples were obtained 24 hours after CLP or LPS injection. Acute phase proteins, cytokines, and chemokines in plasma were determined via MultiAnalyte Profile testing (Rules Based Medicine, Austin, TX). Levels of serum ALT and creatinine were measured with a standard UV method using a Hitachi type 7170 automatic analyzer (Tokyo, Japan).

Measurement of Culture Supernatant. Levels of cytokines (TNF-α, IL-6, IL-10, and IFN-γ) in the culture supernatants were measured using commercially available ELISA kits in accordance with the manufacturer's instructions (BD Biosciences-Pharmingen, San Diego, CA). Haptoglobin was determined in cell-free supernatants by using a commercially available ELISA kit (Immunology Constants Laboratory, Newberg, OR).

Western Blot Analysis. The total cellular protein was extracted with the RIPA buffer containing 1% Nonidet P-40, 0.5% sodium deoxycholate, 0.1% SDS, 50 μg/mL aprotinin, 100 μg/mL phenylmethylsulfonyl fluoride, and 50 mM sodium fluoride in phosphate-buffered saline (pH 7.4). Twenty micrograms of protein were separated

via 7.5% SDS-PAGE and blotted onto a polyvinylidene difluoride membrane. After blocking with Tris-buffered saline 0.1% Tween 20 containing 5% skim milk or Blocking One-P (Nacalai Tesque, Kyoto, Japan) for 1 hour at room temperature, the membrane was incubated overnight at 4°C with antibodies to STAT3 or tyrosine^{705}-phosphorylated STAT3 (Cell Signaling Technology, Danvers, MA), respectively. After washing with Tris-buffered saline 0.1% Tween 20, the membrane was incubated with anti–horseradish peroxidase–linked antibody for 1 hour at room temperature. The immune complex was detected by an enhanced chemiluminescent assay. In some experiments, tyrosine^{701}-phosphorylated STAT1 antibody (Cell Signaling Technology) was also used. This antibody recognizes the phosphorylated form of both STAT1α and STAT1β.

Histology and Terminal Deoxynucleotidyl Transferase-Mediated dUTP Nick End-Labeling. The formalin-fixed livers were paraffin-embedded, and liver sections were analyzed by hematoxylin-eosin staining. Terminal deoxynucleotidyl transferase-mediated deoxyuridine triphosphate nick-end labeling (TUNEL) was performed using an ApopTag kit according to the manufacturer's instructions (Serological Corporation, Norcross, GA).

Primary Culture of Hepatocytes. Livers were digested using a standard in situ 2-step collagenase perfusion procedure (Gibco BRL, Rockville, MD). Hepatocytes were isolated from nonparenchymal cells via subsequent centrifugation at 50*g* for 1 minute. In a selected experiment, nonparenchymal cells in the supernatants were pelleted at 1,500 rpm for 5 minutes and subjected to western blot analysis. Isolated hepatocytes with >90% viability were cultured in Williams' medium E containing 10% fetal bovine serum overnight. On the next day, the cells were stimulated with recombinant IL-6 (PeproTech, London, UK). The cells were harvested after 2 hours for the analysis of STAT3 activation. In another experiment, supernatants were harvested after 48 hours.

Cytokine Production by Macrophage and Splenocytes. The murine macrophage cell line RAW 264.7 was obtained from the American Type Culture Collection (Manassas, VA). RAW cells were plated at a density of 5×10^5/well in a 96-well plate and were incubated at 37°C in culture supernatants of hepatocyte from L-STAT3 KO mice or control mice. As a control, RAW cells were also cultured in Williams' medium E. After 24 hours, LPS was added to achieve a final concentration of 100 ng/mL. After 24 hours of incubation at 37°C in an atmosphere of 5% CO_2, the supernatant was collected and stored at −80°C for measurement of TNF-α, IL-6, and IL-10. Splenocytes were isolated by way of a standard procedure for wild-type mice[17] and incubated with hepatocyte culture supernatant. Twenty-four hours after incubation, the cells were stimulated with LPS (1,000 ng/mL) for 24 hours. The resultant culture supernatant was subjected to IFN-γ ELISA.

Statistics. Kaplan-Meier curves were used to show survival over time. Data are expressed as interquartile range and median and compared using the Mann-Whitney *U* test. Statistical significance was set at $P < 0.05$.

Results

Mice with hepatocyte-specific STAT3 deficiency were produced by crossing floxed STAT3 mice and Alb-Cre transgenic mice carrying the Cre recombinase gene under the regulation of the albumin gene promoter. L-STAT3 KO mice were born and grew without any gross abnormality. Western blot analysis revealed that STAT3 expression was substantially decreased in the liver but not in other organs (Fig. 1A). Isolation of hepatocytes from nonparenchymal cells by liver perfusion followed by centrifugation confirmed that STAT3 deficiency is specific in hepatocytes (Fig. 1B). In addition, STAT3 expression did not differ in peritoneal macrophages between L-STAT3 KO mice and control littermates (Fig. 1C). Those cells isolated from L-STAT3 KO mice produced similar levels of TNF-α in response to LPS compared with those from control littermates (Fig. 1D).

L-STAT3 KO Mice Are More Vulnerable to Septic Shock. To examine the role of hepatic STAT3 during septic shock, we used a well-examined clinically relevant murine model of sepsis performed by CLP.[16] CLP clearly activated liver STAT3, which was determined via phosphorylation of STAT3 in control mice (Fig. 2A), in agreement with a previous report.[18] Liver STAT3 activation during sepsis is mostly due to the activation of STAT3 in hepatocytes, because liver STAT3 was only marginally activated in L-STAT3 KO mice. CLP activated liver STAT1 both in L-STAT3 KO mice and wild-type mice, suggesting that the absence of STAT3 does not affect the activation of other STATs. Given that STAT3 is a well-known mediator for APP,[19] we measured APPs such as fibrinogen and haptoglobin in plasma after CLP (Fig. 2B). The levels of fibrinogen and haptoglobin clearly increased after CLP in wild-type mice. In contrast, induction of fibrinogen was completely diminished in L-STAT3 KO mice, whereas that of haptoglobin was partially inhibited. This is consistent with the previous notion that fibrinogen is a class 2 gene and haptoglobin is a class 1 gene; the class 2 gene is predominantly regulated by type 2 IL-6 responsive elements binding to STAT[20] and the class 1 gene by both type 1 IL-6 responsive elements

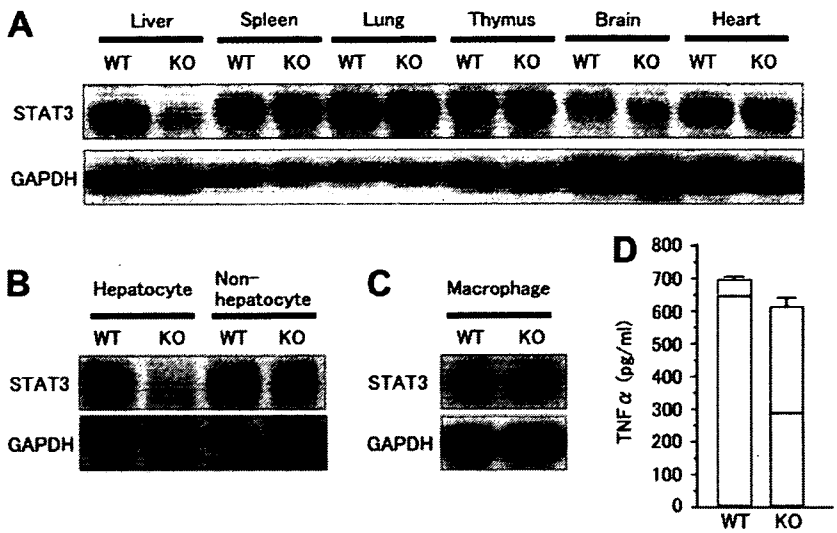

Fig. 1. Hepatocyte-specific STAT3 deficiency in mice. Floxed STAT3 mice were crossed with Alb-Cre transgenic mice. Floxed STAT3 mice having the Alb-Cre transgene were regarded as L-STAT3 KO mice (KO); those not having the Alb-Cre gene were used as a wild-type control (WT). (A) STAT3 expression in a variety of organs from L-STAT3 KO mice and wild-type mice via western blot analysis. Expression of GAPDH was served as a loading control. Representative blots are shown. (B) Expression of STAT3 of isolated hepatocytes and nonhepatocytes. Liver of L-STAT3 KO mice or wild-type mice was collagenase-perfused and separated into hepatocyte and nonhepatocyte fractions. STAT3 expression was determined via western blot analysis. Expression of GAPDH was served as a loading control. Representative blots are shown. (C) Expression of STAT3 in isolated macrophage. Peritoneal macrophage was isolated from L-STAT3 KO mice or wild-type mice and subjected to western blot analysis of STAT3 expression. Representative blots are shown. (D) LPS-stimulated TNF-α production of peritoneal macrophages. Peritoneal macrophages were isolated from L-STAT3 KO mice or wild-type mice ($n = 6$ for each group) and stimulated with LPS (100 ng/mL) for 24 hours. TNF-α production was determined via ELISA in culture supernatants.

binding to CCAAT enhancer-binding protein (C/EBP) and type 2 IL-6 responsive elements.[21]

To address the issue of whether hepatic STAT3 is involved in the outcome of CLP-induced lethality, we performed CLP blinded to the genetic background and checked the survival of the mice every 6 hours. L-STAT3 KO mice were significantly more vulnerable to CLP-induced lethality than wild-type littermates (Fig. 2C). To examine the possible difference in bacterial infection after CLP, we measured colony forming unit of blood bacteria 24 hours after CLP. Because there was no significant difference in bacterial amount between L-STAT3 KO mice and wild-type mice (Fig. 2D), we considered hepatic STAT3 to have had a beneficial effect on the outcome of septic shock without affecting bacterial infection.

Hepatic STAT3-Deficient Mice Show Exacerbated Liver Injury. To examine liver injury and renal dysfunction in CLP-induced sepsis, we measured ALT and creatinine levels. L-STAT3 KO mice showed increased levels of serum ALT and creatinine compared with wild-type littermates, although the difference in creatinine did not reach a significant level (Fig. 3A). TUNEL of the liver revealed that the number of apoptotic hepatocytes was significantly higher in L-STAT3 KO mice than in wild-type littermates (Fig. 3B,C). However, the liver injury itself presumably is not a direct cause of animal death, because histologic abnormality was modest. Furthermore, LPS injection, which is another model of septic shock, induced more hepatocyte apoptosis than CLP but did not kill any mice tested (Fig. 3A-C and data not shown), supporting the idea that increased liver injury could not explain the increased lethality in L-STAT3 KO mice.

Exacerbated Systemic Inflammatory Response in L-STAT3 KO Mice. Hypercytokinemia underlying systemic inflammatory response syndrome may play an important role in the development of multiple organ dysfunction syndrome and lethality.[9] We measured several circulating cytokines and chemokines in septic mice and found that TNF-α, IFN-γ, IL-6, IL-10, monocyte chemoattractant protein-1 (MCP-1) and macrophage inflammatory protein-1β (MIP-1β) had clearly increased 24 hours after CLP in L-STAT3 KO mice. Of importance is the finding that the plasma levels of these cytokines and chemokines were significantly higher in L-STAT3 KO mice than in wild-type mice, although they did not differ before CLP. This result indicates that the increased lethality found in L-STAT3 KO mice is associated with hypercytokinemia (Fig. 4A). Although plasma insulin levels significantly increased 24 hours after CLP, there was no significant difference between L-STAT3 KO mice and wild-type mice, suggesting that insulin levels do not affect the difference in animal lethality (Supplementary Fig. 1).

Given that bacterial infection did not differ between L-STAT3 KO mice and wild-type mice, we examined the

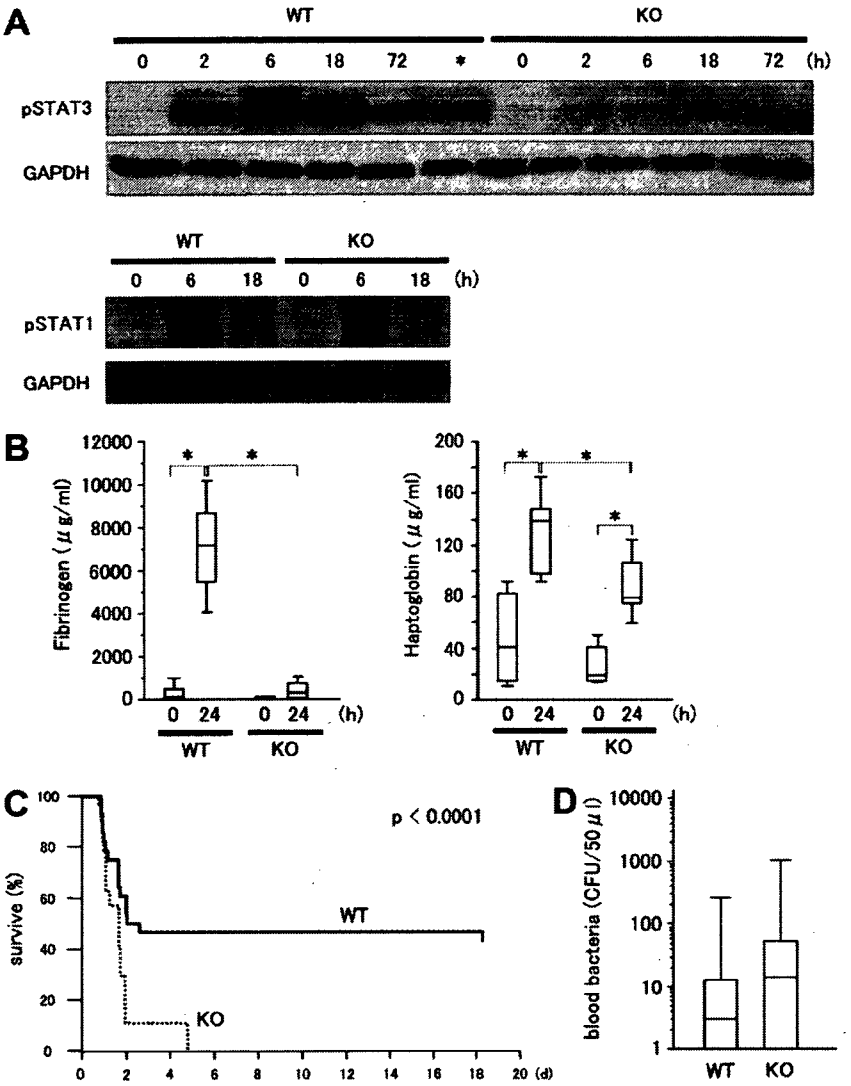

Fig. 2. STAT3 activation, APP production, and survival in CLP mice. (A) Western blot analysis of phosphorylated STAT3 and STAT1 in CLP mice. L-STAT3 KO mice (KO) and wild-type mice (WT) were treated with CLP and sacrificed at the indicated time points. Their liver tissues were subjected to analysis of Tyrosine 705 phosphorylation of STAT3 or Tyrosine 701 phosphorylation of STAT1 via western blot analysis. GAPDH expression served as a control. Representative blots are shown. *7 days. (B) Levels of circulating haptoglobin and fibrinogen before and 24 hours after CLP (n = 8 for each group). *$P < 0.05$. (C) Comparison of survival after CLP between L-STAT3 KO (n = 27) mice and wild-type littermates (n =28). (D) Colony-forming units of blood bacteria after CLP. L-STAT3 KO or wild-type mice were sacrificed 24 hours after CLP. Blood samples were subjected to analysis of bacterial growth (n = 10 for knockout mice and n = 9 for wild-type mice).

response of cytokine production upon endotoxin stimulation. To this end, we injected the same amount of LPS to L-STAT3 KO mice and control mice and measured circulating cytokines. LPS injection into L-STAT3 KO mice upregulated those cytokines to a lesser extent than CLP. In agreement with the finding on the CLP model, the levels of TNF-α, IL-10, MCP-1, and MIP-1β were significantly higher in L-STAT3 KO mice than in wild-type mice after LPS injection (Fig. 4B), indicating that L-STAT3 KO mice were highly sensitive to endotoxin and prone to show hypercytokinemia.

STAT3-Regulated Soluble Factors Produced by Hepatocytes Suppress Cytokine Production From Immune Cells. To examine the underlying mechanisms of the hyperimmune response in L-STAT3 KO mice, we hypothesized that STAT3-mediated soluble factors from hepatocytes repress cytokine production from immune cells. We isolated hepatocytes from L-STAT3 KO mice and control mice and stimulated them with or without IL-6, collecting the conditional medium of hepatocytes. Wild-type hepatocytes displayed STAT3 activation in primary culture without stimulation, but the levels increased upon IL-6 exposure, whereas KO hepatocytes did not show any STAT3 activation (Fig. 5A). Consistent with this was the finding that the wild-type hepatocytes produced more haptoglobin than KO hepatocytes, even in the absence of IL-6 (Fig. 5B).

Next, we cultured RAW cells, a murine macrophage cell line, in the presence or absence of culture supernatant of hepatocytes. RAW cells produced TNF-α, IL-6, and IL-10 but not IFN-γ upon stimulation of LPS, and hepatocyte culture supernatant suppressed the production of these cytokines (Fig. 5C). Importantly, the suppression was significantly weaker in the presence of conditional medium of KO hepatocytes than in the presence of conditional medium of wild-type hepato-

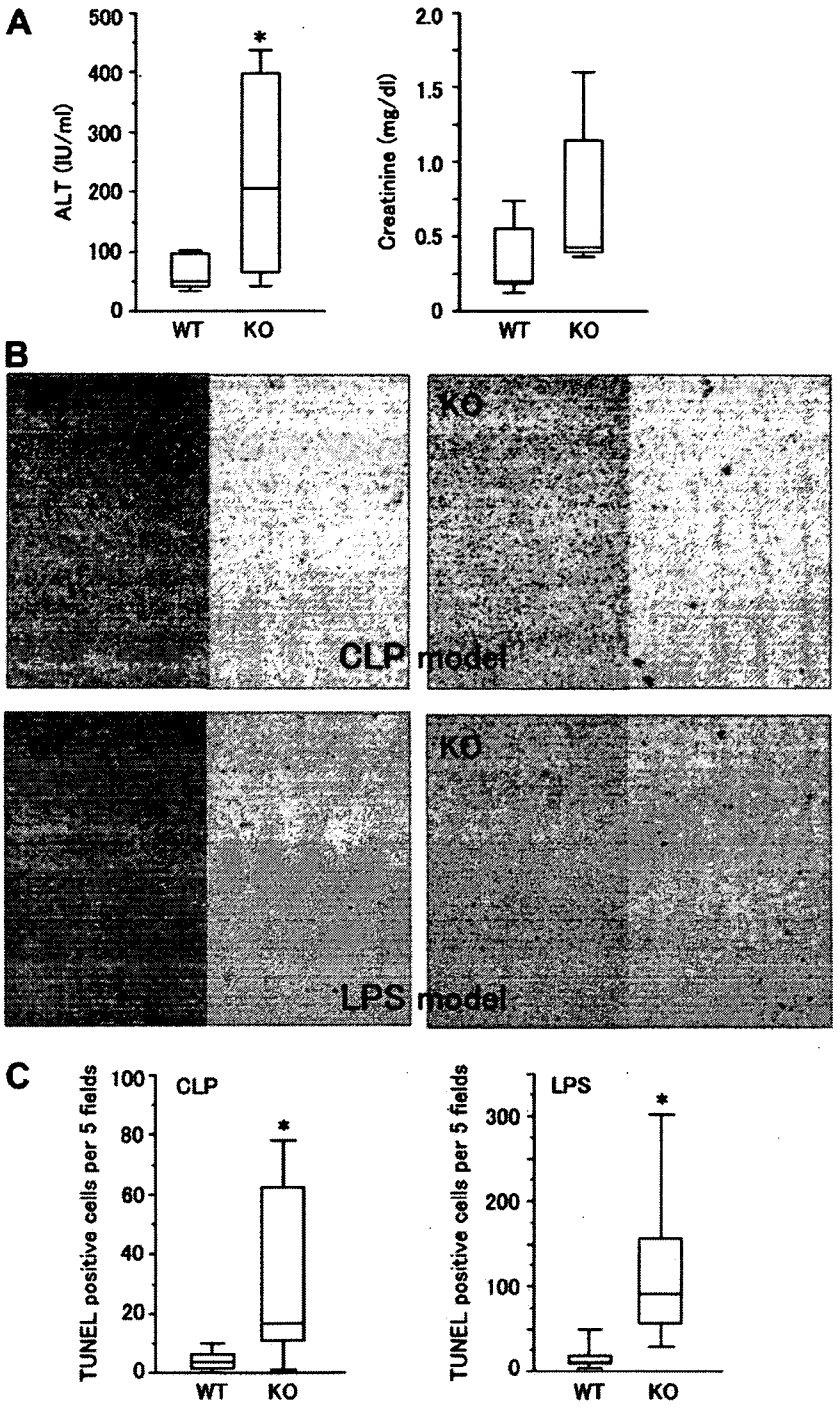

Fig. 3. Organ injury in septic mice. (A) Serum ALT and creatinine levels in L-STAT3 KO mice (KO) and control mice (WT) 24 hours after CLP. $*P < 0.05$. (B) Representative histology (left part of each panel) and TUNEL (right part of each panel) of liver sections 24 hours after CLP or LPS injection. (C) Comparison of TUNEL-positive hepatocytes for at least 9 mice in each group. $*P < 0.05$.

cytes. Furthermore, murine primary splenocytes produced IFN-γ upon LPS stimulation, and the production was also suppressed in the presence of conditional medium of hepatocytes. Again, IFN-γ production was significantly higher in splenocytes cultured with KO hepatocyte supernatant than in those with wild-type hepatocyte supernatant (Fig. 5D). These data indicate that soluble substances from hepatocytes suppressed activation of immune cells, which was critically dependent on STAT3.

Discussion

The present study clearly demonstrated that the absence of STAT3 in hepatocytes leads to high levels of circulating cytokines and increased mortality of CLP-in-

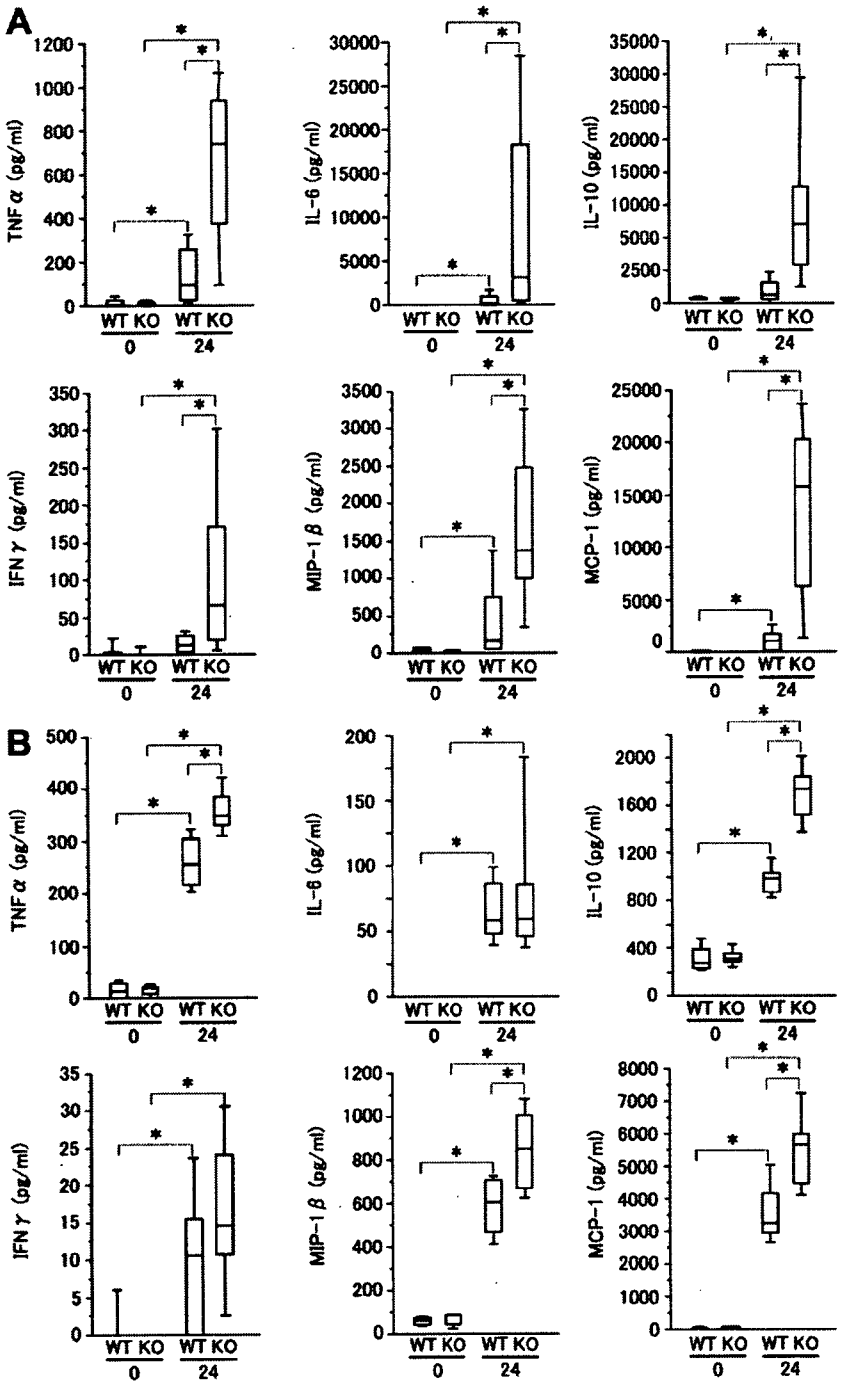

Fig. 4. Circulating cytokines before and after CLP or LPS injection. (A) L-STAT3 KO mice (KO) or wild-type littermates (WT) were treated with CLP (n = 8 in each group). Before and 24 hours after CLP, blood samples were obtained from mice and subjected to analysis of each cytokine indicated. *$P < 0.05$. (B) Mice were injected with 4 mg/kg of LPS (n = 8 in each group). Before and 24 hours after LPS injection, blood samples were obtained and subjected to the analysis of each cytokine indicated. *$P < 0.05$.

duced septic mice without affecting bacterial infection. L-STAT3 KO mice produced high levels of cytokines when injected with LPS, confirming that the absence of STAT3 signaling within hepatocytes induces a hyperinflammatory response even if the extent of the input stimuli remains constant. This phenomenon is similar to a previous report of macrophage-specific disruption of STAT3 in which serum cytokines such as TNF-α, IL-6, and IL-10 increased upon LPS stimulation.[22] In those mice, immune cells could not respond to IL-10, which potentially inhibit TNF-α production via STAT3 signaling, and thus produced high levels of TNF-α. Further study revealed those mice to be vulnerable to CLP-induced sepsis.[23,24] However, in our L-STAT3 KO mice, the levels of STAT3 in macrophage did not differ from control mice and produced the same amount of TNF-α in response to LPS (Fig. 1C-D). Thus, suppression of the inflammatory response in wild-type mice was critically

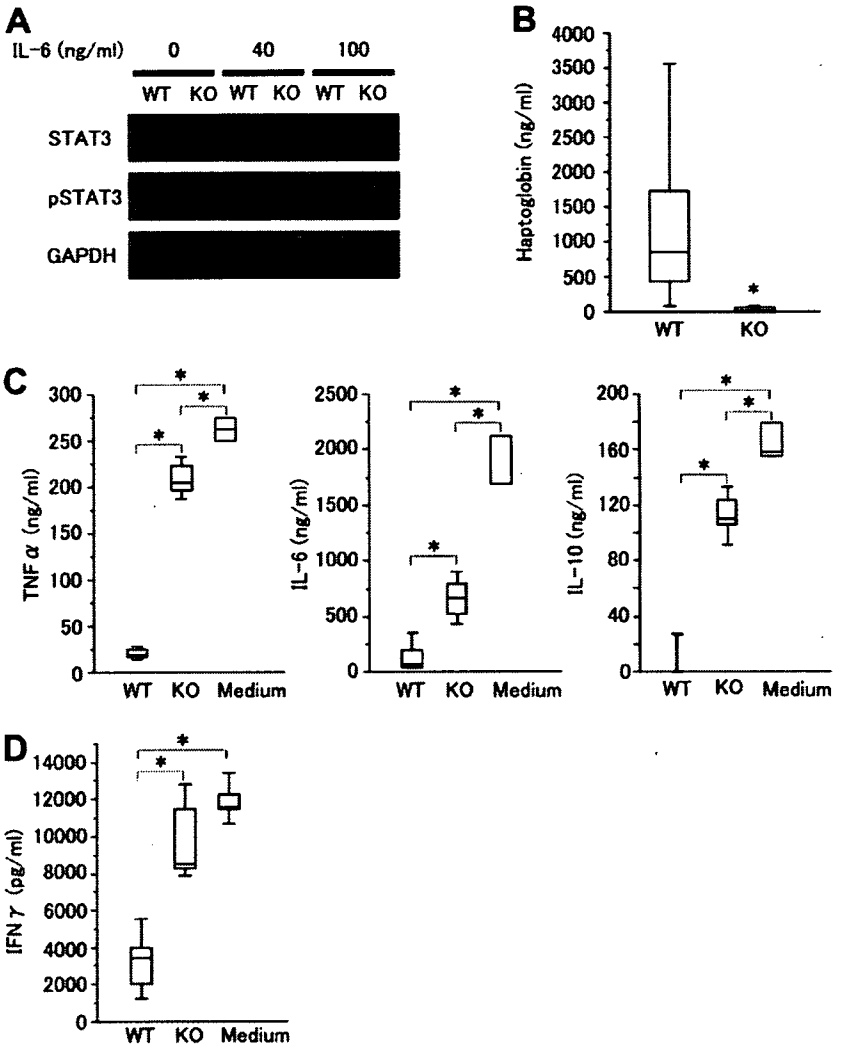

Fig. 5. Suppression of cytokine production from immune cells by hepatocyte culture supernatant. Hepatocytes were isolated from L-STAT3 KO (KO) or wild-type (WT) mice and cultured in the presence or absence of IL-6 for 2 hours (for western blot analysis) or 48 hours (for collection of culture supernatants). (A) STAT3 phosphorylation (pSTAT3) and STAT3 expression of hepatocytes via western blot analysis. GAPDH expression served as a control. Representative blots are shown. (B) Haptoglobin production from primary hepatocytes. Haptoglobin concentration was determined in the hepatocyte supernatants via ELISA. Comparison of haptoglobin production between knockout hepatocytes and wild-type hepatocytes ($n = 5$ mice/group) cultured in the absence of IL-6. $^*P < 0.05$. (C,D) Suppression of cytokine production in RAW cells or splenocytes by the hepatocyte supernatants. Hepatocytes were cultured for 48 hours. RAW cells (C) or splenocytes freshly isolated from wild-type mice (D) were cultured in the presence (KO or WT) or absence (Medium) of hepatocyte supernatants for 24 hours and then stimulated with LPS for another 24 hours. TNF-α, IL-6, IL-10, and IFN-γ production was determined via ELISA. $^*P < 0.05$.

dependent on hepatic STAT3 signaling. Indeed, in vitro analysis revealed that soluble factors from hepatocytes repress cytokine production from activated macrophage and splenocytes in a hepatic STAT3-dependent manner. Whereas research has established that STAT3 mediates a variety of effects on hepatocytes, including proliferation,[5] apoptosis protection,[6] and glucose metabolism,[7] the present study reveals that hepatic STAT3 has an important extrahepatic effect. This effect is activated by a variety of cytokines produced from immune cells such as IL-6 but, in turn, suppresses immune cell activation via production of soluble factors, providing a negative feedback loop. Thus, the present study describes a role of hepatic STAT3 in maintaining host homeostasis by negatively regulating the immune system.

APPs are liver plasma proteins whose levels of expression are either positively or negatively regulated by cytokines during inflammation. It has been established that STAT3 regulates the expression of most, if not all, APPs in the liver.[19] Consistent with this, L-STAT3 KO mice displayed impaired production of APPs in response to CLP (Fig. 2B). Some APPs such as C-reactive protein,[25] serum amyloid P,[26] and α2-macroglobulin[27] have been shown to bind bacteria and to positively or negatively affect their eradication. Several reports also suggest that APPs exert proinflammatory as well as anti-inflammatory effects.[25,28] C-reactive protein binds to the phosphocholine of some foreign pathogens as well as phospholipid constituents of damaged cells and can activate the complement system, whereas the antioxidants haptoglobin and hemopexin protect against reactive oxygen species. Thus, each APP has a unique role in the complex mechanism controlling infection-induced inflammation. The L-STAT3 KO mice used in the present study offer a unique model for identifying the net effect of STAT3-regulated APPs during the septic condition. Our work has revealed that the most prominent effect of STAT3-regulated APPs is suppression of the hyperinflammatory re-

sponse and lethality without an effect on bacterial infection. The soluble factors from hepatocytes that suppress cytokine production from immune cells are still unknown. Although there may be several substances involved in this phenomenon, one candidate might be haptoglobin, which was recently demonstrated to suppress TNF-α, IL-12, and IL-10 from human peripheral blood mononuclear cells in vitro.[29] We also obtained a similar finding that RAW cells produced a lesser amount of TNF-α upon LPS stimulation in the presence of haptoglobin (Supplementary Fig. 2). Identification of these substances may have important therapeutic implications for controlling the hyperinflammatory condition. Further study is needed to clarify this point.

The liver is one of the target organs of sepsis-induced multiple organ dysfunction syndrome. Evidence for this comes from the fact that CLP mice or LPS mice showed liver injury as evidenced by increases in serum ALT and TUNEL-positive hepatocytes scattered in the liver lobule. Furthermore, L-STAT3 KO mice displayed more hepatocyte apoptosis in mice subjected to CLP or LPS injection. Previous research has indicated that the absence of hepatic STAT3 renders hepatocytes more vulnerable to Fas-mediated apoptosis.[6] It is possible that STAT3-null hepatocytes are more vulnerable to apoptosis in the septic model. However, at the same time, L-STAT3 KO mice showed higher levels of proinflammatory cytokines such as TNF-α, which is a direct inducer of hepatocyte apoptosis. In our model, it is difficult to differentiate which contributed more to increased liver injury: the decrease in apoptosis resistance or the increase in proinflammatory cytokine. It can be said that the increase of proinflammatory cytokines is presumably one of the causes, but not a result, of liver injury. In addition, as discussed in the Results section, liver injury was relatively modest and probably not a direct cause of animal death.

In the present study, the lack of hepatic STAT3 caused increased mortality in CLP mice. Although we did not address the direct link between hypercytokinemia and animal death, accumulating evidence suggests that an increase in a variety of cytokines is involved in lethality in CLP mice. For example, it was shown that IL-6 plays an important role in the increased expression of the C5a receptor in the lung, liver, kidney, and heart during the development of sepsis in CLP mice and that interception of IL-6 leads to reduced expression of the C5a receptor and improved survival.[30] In addition, enforced expression of the IL-6 gene in wild-type mice led to high mortality (unpublished data). TNF-α and other cytokines increase expression of inducible nitric oxide synthase, and increased production of nitric oxide causes further vascular instability and may also contribute to the direct myocardial depression that occurs in sepsis.[31] Thus, dysregulation of cytokines may be harmful for host organs and is probably linked to animal death.

The present study revealed an important role of hepatocytes in repressing the hyperinflammatory response in pathologic conditions. This raises the possibility that hyperinflammation may be ill-controlled when liver function is severely impaired. Although sepsis itself is not a frequent cause of liver failure, it is a serious complication of acute or chronic liver failure. Systemic inflammatory response syndrome is an important determinant of prognosis in fulminant hepatitis.[12] Sepsis originating from spontaneous bacterial peritonitis or renal infection is one of the causes of patient death with decompensated cirrhosis.[13] In patients with limited function of the liver, possible impairment of STAT3-regulated hepatocyte function may be involved in their poor prognosis when complicated with severe inflammation. Careful liver-supporting therapy or early liver transplantation should be considered not only for maintaining liver function but also from the aspect of controlling dysregulated hyperinflammatory responses.

In conclusion, hepatic STAT3 represses systemic hyperinflammatory response by stimulating hepatic production of soluble substances that can attenuate immune cell overactivation and also improves host survival during septic condition. This sheds light on hepatocytic STAT3 as a negative regulator for immune cell overactivation and its role in host defense during systemic severe inflammation.

References

1. Akira S. IL-6-regulated transcription factors. Int J Biochem Cell Biol 1997; 29:1401-1418.
2. Akira S, Nishio Y, Inoue M, Wang XJ, Wei S, Matsusaka T, et al. Molecular cloning of APRF, a novel IFN-stimulated gene factor 3 p91-related transcription factor involved in the gp130-mediated signaling pathway. Cell 1994;77:63-71.
3. Zhong Z, Wen Z, Darnell JE Jr. Stat3: a STAT family member activated by tyrosine phosphorylation in response to epidermal growth factor and interleukin-6. Science 1994;264:95-98.
4. Takeda K, Noguchi K, Shi W, Tanaka T, Matsumoto M, Yoshida N, et al. Targeted disruption of the mouse Stat3 gene leads to early embryonic lethality. Proc Natl Acad Sci U S A 1997;94:3801-3804.
5. Li W, Liang X, Kellendonk C, Poli V, Taub R. STAT3 contributes to the mitogenic response of hepatocytes during liver regeneration. J Biol Chem 2002;277:28411-28417.
6. Haga S, Terui K, Zhang HQ, Enosawa S, Ogawa W, Inoue H, et al. Stat3 protects against Fas-induced liver injury by redox-dependent and -independent mechanisms. J Clin Invest 2003;112:989-998.
7. Inoue H, Ogawa W, Ozaki M, Haga S, Matsumoto M, Furukawa K, et al. Role of STAT-3 in regulation of hepatic gluconeogenic gene and carbohydrate metabolism in vivo. Nat Med 2004;10:168-174.
8. Angus DC, Linde-Zwirble WT, Lidicker J, Clermont G, Carcillo J, Pinsky MR. Epidemiology of severe sepsis in the United States: analysis of incidence, outcome, and associated costs of care. Crit Care Med 2001;29: 1303-1310.
9. Cohen J. The immunopathogenesis of sepsis. Nature 2002;420:885-891.

10. Hotchkiss RS, Karl IE. The pathophysiology and treatment of sepsis. N Engl J Med 2003;348:138-150.
11. Wang P, Chaudry IH. Mechanism of hepatocellular dysfunction during hyperdynamic sepsis. Am J Physiol 1996;270:R927-R938.
12. Rolando N, Wade J, Davalos M, Wendon J, Philpott-Howard J, Williams R. The systemic inflammatory response syndrome in acute liver failure. HEPATOLOGY 2000;32:734-739.
13. Fasolato S, Angeli P, Dallagnese L, Maresio G, Zola E, Mazza E, et al. Renal failure and bacterial infections in patients with cirrhosis: epidemiology and clinical features. HEPATOLOGY 2007;45:223-229.
14. Takeda K, Kaisho T, Yoshida N, Takeda J, Kishimoto T, Akira S. Stat3 activation is responsible for IL-6-induced T cell proliferation through preventing apoptosis: generation and characterization of T cell-specific Stat3-deficient mice. J Immunol 1998;161:4652-4660.
15. Takehara T, Tatsumi T, Suzuki T, Rucker EB 3rd, Hennighausen L, Jinushi M, et al. Hepatocyte-specific disruption of Bcl-xL leads to continuous hepatocyte apoptosis and liver fibrotic responses. Gastroenterology 2004;127:1189-1197.
16. Fink MP, Heard SO. Laboratory models of sepsis and septic shock. J Surg Res 1990;49:186-196.
17. Takehara T, Uemura A, Tatsumi T, Suzuki T, Kimura R, Shiotani A, et al. Natural killer cell-mediated ablation of metastatic liver tumors by hydrodynamic injection of IFNα gene to mice. Int J Cancer 2007;120:1252-1260.
18. Andrejko KM, Chen J, Deutschman CS. Intrahepatic STAT-3 activation and acute phase gene expression predict outcome after CLP sepsis in the rat. Am J Physiol 1998;275:G1423-G1429.
19. Alonzi T, Maritano D, Gorgoni B, Rizzuto G, Libert C, Poli V. Essential role of STAT3 in the control of the acute-phase response as revealed by inducible gene inactivation in the liver. Mol Cell Biol 2001;21:1621-1632.
20. Zhang Z, Fuentes NL, Fuller GM. Characterization of the IL-6 responsive elements in the gamma fibrinogen gene promoter. J Biol Chem 1995;270:24287-24291.
21. Kim H, Baumann H. The carboxyl-terminal region of STAT3 controls gene induction by the mouse haptoglobin promoter. J Biol Chem 1997;272:14571-14579.
22. Takeda K, Clausen BE, Kaisho T, Tsujimura T, Terada N, Forster I, et al. Enhanced Th1 activity and development of chronic enterocolitis in mice devoid of Stat3 in macrophages and neutrophils. Immunity 1999;10:39-49.
23. Matsukawa A, Takeda K, Kudo S, Maeda T, Kagayama M, Akira S. Aberrant inflammation and lethality to septic peritonitis in mice lacking STAT3 in macrophages and neutrophils. J Immunol 2003;171:6198-6205.
24. Matsukawa A, Kudo S, Maeda T, Numata K, Watanabe H, Takeda K, et al. Stat3 in resident macrophages as a repressor protein of inflammatory response. J Immunol 2005;175:3354-3359.
25. Gabay C, Kushner I. Acute-phase proteins and other systemic responses to inflammation. N Engl J Med 1999;340:448-454.
26. Noursadeghi M, Bickerstaff MC, Gallimore JR, Herbert J, Cohen J, Pepys MB. Role of serum amyloid P component in bacterial infection: protection of the host or protection of the pathogen. Proc Natl Acad Sci U S A 2000;97:14584-14589.
27. Hochepied T, Van Leuven F, Libert C. Mice lacking alpha2-macroglobulin show an increased host defense against Gram-negative bacterial sepsis, but are more susceptible to endotoxic shock. Eur Cytokine Netw 2002;13:86-91.
28. Tilg H, Dinarello CA, Mier JW. IL-6 and APPs: anti-inflammatory and immunosuppressive mediators. Immunol Today 1997;18:428-432.
29. Arredouani MS, Kasran A, Vanoirbeek JA, Berger FG, Baumann H, Ceuppens JL. Haptoglobin dampens endotoxin-induced inflammatory effects both in vitro and in vivo. Immunology 2005;114:263-271.
30. Riedemann NC, Neff TA, Guo RF, Bernacki KD, Laudes IJ, Sarma JV, et al. Protective effects of IL-6 blockade in sepsis are linked to reduced C5a receptor expression. J Immunol 2003;170:503-507.
31. Landry DW, Oliver JA. The pathogenesis of vasodilatory shock. N Engl J Med 2001;345:588-595.

Enhanced TLR-mediated NF-IL6–dependent gene expression by Trib1 deficiency

Masahiro Yamamoto,[1,3] Satoshi Uematsu,[1] Toru Okamoto,[2] Yoshiharu Matsuura,[2] Shintaro Sato,[4] Himanshu Kumar,[1] Takashi Satoh,[1,4] Tatsuya Saitoh,[1] Kiyoshi Takeda,[3,5] Ken J. Ishii,[4] Osamu Takeuchi,[1,4] Taro Kawai,[1,4] and Shizuo Akira[1,4]

[1]Department of Host Defense and [2]Department of Molecular Virology, Research Institute for Microbial Diseases and [3]Department of Microbiology and Immunology, Graduate School of Medicine, Osaka University, Suita, Osaka 565-0871, Japan
[4]Exploratory Research for Advanced Technology, Japan Science and Technology Corporation, Suita, Osaka, 565-0871, Japan
[5]Department of Embryonic and Genetic Engineering, Medical Institute of Bioregulation, Kyushu University, Higashi-ku, Fukuoka 812-8582, Japan

Toll-like receptors (TLRs) recognize a variety of microbial components and mediate downstream signal transduction pathways that culminate in the activation of nuclear factor κB (NF-κB) and mitogen-activated protein (MAP) kinases. Trib1 is reportedly involved in the regulation of NF-κB and MAP kinases, as well as gene expression in vitro. To clarify the physiological function of Trib1 in TLR-mediated responses, we generated Trib1-deficient mice by gene targeting. Microarray analysis showed that Trib1-deficient macrophages exhibited a dysregulated expression pattern of lipopolysaccharide-inducible genes, whereas TLR-mediated activation of MAP kinases and NF-κB was normal. Trib1 was found to associate with NF-IL6 (also known as CCAAT/enhancer-binding protein β). NF-IL6–deficient cells showed opposite phenotypes to those in Trib1-deficient cells in terms of TLR-mediated responses. Moreover, overexpression of Trib1 inhibited NF-IL6–dependent gene expression by down-regulating NF-IL6 protein expression. In contrast, Trib1-deficient cells exhibited augmented NF-IL6 DNA-binding activities with increased amounts of NF-IL6 proteins. These results demonstrate that Trib1 is a negative regulator of NF-IL6 protein expression and modulates NF-IL6–dependent gene expression in TLR-mediated signaling.

CORRESPONDENCE
Shizuo Akira:
sakira@biken.osaka-u.ac.jp

Abbreviations used: 24p3, lipocalin-2; BLP, bacterial lipoprotein; C/EBP, CCAAT/enhancer-binding protein; Jnk, c-Jun N-terminal kinase; MALP-2, macrophage-activating lipopeptide-2; MAP, mitogen-activated protein; mPGES, prostaglandin E synthase; TLR, Toll-like receptor.

Innate immunity is promptly activated after the invasion of microbes through recognition of pathogen-associated molecular patterns by pattern-recognition receptors, including Toll-like receptors (TLRs) (1). The recognition of microbial components by TLRs effectively stimulates host immune responses such as proinflammatory cytokine production, cellular proliferation, and up-regulation of co-stimulatory molecules, accompanied by the activation of NF-κB and mitogen-activated protein (MAP) kinases (2, 3). Although the inhibitory protein IκB family members sequester NF-κB in the cytoplasm of unstimulated cells, TLR-dependent IκB phosphorylation by the IκB kinase complex and degradation by the ubiquitin–proteasome pathway permit translocation of NF-κB to the nucleus (4). MAP kinases such as c-Jun N-terminal kinase (Jnk) and p38 are also rapidly phosphorylated and activated by upstream kinases in response to TLR stimulation (5). Moreover, TLR-mediated activity of NF-κB and MAP kinases is shown to be regulated at multiple steps regarding the strength and the duration of the activation (6).

Recent extensive experiments have identified a variety of modulators that have positive and negative effects on the activation of NF-κB and MAP kinases, including a family of serine/threonine kinase-like proteins called Trib (7). Trib consists of three family members: Trib1 (also known as c8fw, GIG2, or SKIP1), Trib2 (also known as c5fw), and Trib3 (also known as NIPK, SINK, or SKIP3) (7–12). Trib3 has been shown to interact with the p65 subunit of NF-κB and to inhibit NF-κB–dependent gene expression in vitro (11). In terms of MAP kinases, Trib1, Trib2, and Trib3 reportedly bind to Jnk and p38, and affect the activity of MAP kinases and IL-8 production in response to PMA or

The online version of this article contains supplemental material.

JEM © The Rockefeller University Press $30.00
Vol. 204, No. 9, September 3, 2007 2233-2239 www.jem.org/cgi/doi/10.1084/jem.20070183

TLR ligands/IL-1 (12). However, whether Trib family members regulate TLR-mediated signaling pathways under physiological conditions is still unknown.

In this study, we generated Trib1-deficient mice by gene targeting and analyzed TLR-mediated responses. Although the activation of NF-κB and MAP kinases in response to LPS was comparable between wild-type and Trib1-deficient cells, microarray analysis revealed that a subset of LPS-inducible genes was dysregulated in Trib1-deficient cells. Subsequent yeast two-hybrid analysis identified the CCAAT/enhancer-binding protein (C/EBP) family member NF-IL6 (also known as C/EBPβ) as a binding partner of Trib1, and phenotypes found in NF-IL6–deficient cells were opposite to those observed in Trib1-deficient cells. Moreover, overexpression of Trib1 inhibited NF-IL6–mediated gene expression and reduced amounts of NF-IL6 proteins. Inversely, NF-IL6 DNA-binding activity and LPS-inducible NF-IL6–target gene expression were up-regulated in Trib1-deficient cells, in which amounts of NF-IL6 proteins were increased. These results demonstrate that Trib1 plays an important role in NF-IL6–dependent gene expression in the TLR-mediated signaling pathways.

RESULTS

Comprehensive gene expression analysis in Trib1-deficient macrophages

To assess the physiological function of Trib1 in TLR-mediated immune responses, we performed a microarray analysis to compare gene expression profiles between wild-type and Trib1-deficient macrophages in response to LPS (Fig. 1 A and Fig. S1, available at http://www.jem.org/cgi/content/full/jem.20070183/DC1). Out of 45,102 transcripts, we first defined the genes induced more than twofold after LPS stimulation in wild-type cells as "LPS-inducible genes" and identified 790 of them (Table S1). We next compared the LPS-inducible genes in wild-type and Trib1-deficient macrophages after LPS stimulation and found 59, 703, and 28 genes as up-regulated, similarly expressed, and down-regulated in Trib1-deficient cells, respectively (Table S1).

Among the up-regulated genes, several were subsequently tested by Northern blotting to confirm the accuracy. LPS-induced expression of prostaglandin E synthase (mPGES), lipocalin-2 (24p3), arginase type II, and plasminogen activator inhibitor type II, which were highly up-regulated in the microarray analysis (Table S1), was indeed enhanced in Trib1-deficient macrophages (Fig. 1 B). Furthermore, in contrast to proinflammatory cytokines such as TNF-α and IL-6, which were similarly expressed between wild-type and Trib1-deficient cells in response not only to LPS but also to other TLR ligands, IL-12 p40 was down-regulated in Trib1-deficient cells compared with wild-type cells (Fig. 1 C; Fig. S2, A–C, available at http://www.jem.org/cgi/content/full/jem.20070183/DC1; and Table S1). Thus, the comprehensive microarray analysis revealed that a subset of LPS-inducible genes is dysregulated in Trib1-deficient cells.

Previous in vitro studies demonstrate that human Trib family members modulate activation of MAP kinases and

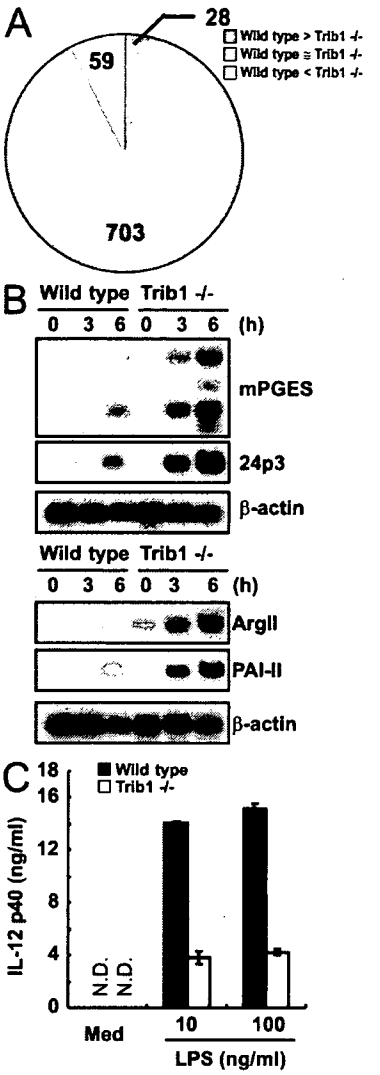

Figure 1. Dysregulation of a subset of LPS-inducible genes in Trib1-deficient cells. (A) Summary of DNA chip microarray analysis. 790 LPS-inducible genes were divided into up-regulated (yellow), similarly expressed (pink), and down-regulated (blue) groups, with the indicated amounts of each. (B) Peritoneal macrophages from wild-type or Trib1-deficient mice were stimulated with 10 ng/ml LPS for the indicated periods. Total RNA (10 μg) was extracted and subjected to Northern blot analysis for the expression of the indicated probes. (C) Peritoneal macrophages from wild-type and Trib1-deficient mice were cultured with the indicated concentrations of LPS in the presence of 30 ng/ml IFN-γ for 24 h. Concentrations of IL-12 p40 in the culture supernatants were measured by ELISA. Indicated values are means ± SD of triplicates. Data are representative of three (B) or two (C) independent experiments. N.D., not detected.

NF-κB (7–12). Both wild-type and Trib1-deficient cells showed similar levels and time courses of phosphorylation of p38, Jnk and extracellular signal-regulated kinase, and IκBα degradation (Fig. S2 D), indicating that the dysregulated

expression of LPS-inducible genes in Trib1-deficient cells might be the independent of activation of NF-κB and MAP kinases.

Interaction of Trib1 with NF-IL6

To explore signaling aspects of Trib1 deficiency other than NF-κB and MAP kinases, we performed a yeast-two-hybrid screen with the full length of human Trib1 as bait to identify a binding partner of Trib1 and identified several clones as being positive. Sequence analysis subsequently revealed that three clones encoded the N-terminal portion of a member of the C/EBP NF-IL6 (unpublished data). We initially tested the interaction of Trib1 and NF-IL6 in yeasts. AH109 cells were transformed with a plasmid encoding the full length of Trib1 together with a plasmid encoding the N-terminal portion of NF-IL6 obtained by the screening (Fig. 2 A). We next examined the interaction in mammalian cells using immunoprecipitation experiments. HEK293 cells were transiently transfected with a plasmid encoding the full length of mouse Trib1 together with a plasmid encoding the full length of mouse NF-IL6. Myc-tagged NF-IL6 was coimmunoprecipitated with Flag-Trib1 (Fig. 2 B), showing the interaction of Trib1 and NF-IL6 in mammalian cells.

TLR-mediated immune responses in NF-IL6–deficient macrophages

An in vitro study showing the interaction of Trib1 and NF-IL6 prompted us to examine the TLR-mediated immune responses in NF-IL6–deficient cells, because LPS-induced expression of mPGES is shown to depend on NF-IL6 (13). We initially analyzed the expression pattern of genes affected by the loss of Trib1 in NF-IL6–deficient macrophages by Northern blotting. LPS-induced expression of 24p3, plasminogen activator inhibitor type II, and arginase type II, as well as mPGES, was profoundly defective in NF-IL6–deficient cells (Fig. 2 C). We next tested IL-12 p40 production by ELISA. As previously reported, IL-12 p40 production by LPS stimulation was increased in a dose-dependent fashion in NF-IL6–deficient cells compared with control cells (Fig. 2 D) (14). In addition, the production in response to bacterial lipoprotein (BLP), macrophage-activating lipopeptide–2 (MALP-2), or CpG DNA was also augmented in

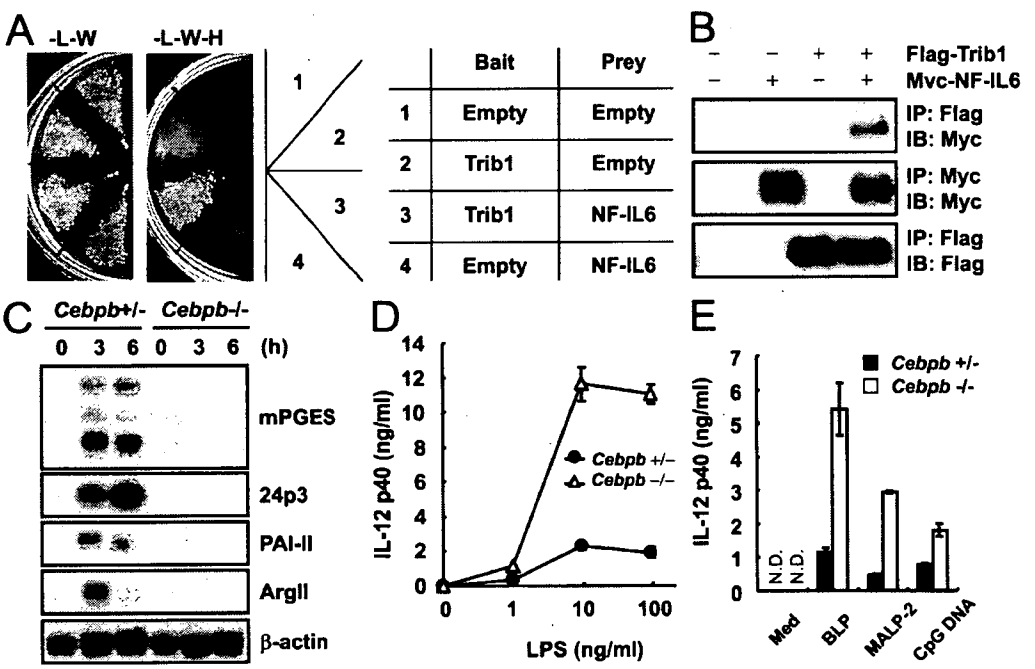

Figure 2. Association of Trib1 with NF-IL6 and TLR-mediated responses in NF-IL6–deficient macrophages. (A) Plasmids expressing human Trib1 fused to the GAL4 DNA-binding domain or an empty vector were cotransfected with a plasmid expressing NF-IL6 fused to GAL4 transactivation domain or an empty vector. Interactions were detected by the ability of cells to grow on medium lacking tryptophan, leucin, and histidine (-L-W-H). The growth of cells on a plate lacking tryptophan and leucine (-L-W) is indicative of the efficiency of the transfection. (B) Lysates of HEK293 cells transiently cotransfected with 2 μg of Flag-tagged Trib1 and/or 2 μg Myc-tagged NF-IL6 expression vectors were immunoprecipitated with the indicated antibodies. (C) Peritoneal macrophages from wild-type or NF-IL6–deficient mice were stimulated with 10 ng/ml LPS for the indicated periods. Total RNA (10 μg) was extracted and subjected to Northern blot analysis for expression of the indicated probes. (D and E) Peritoneal macrophages from wild-type and NF-IL6–deficient mice were cultured with the indicated concentrations of LPS (D) or with 100 ng/ml BLP, 30 ng/ml MALP-2, or 1 μM, CpG DNA (E) in the presence of 30 ng/ml IFN-γ for 24 h. Concentrations of IL-12 p40 in the culture supernatants were measured by ELISA. Indicated values are means ± SD of triplicates. Data are representative of three (B) and two (C–E) separate experiments. N.D., not detected.

NF-IL6–deficient cells (Fig. 2 E). Together, compared with Trib1-deficient cells, converse phenotypes in terms of TLR-mediated immune responses are observed in NF-IL6–deficient cells.

Inhibition of NF-IL6 by Trib1 overexpression

To test whether Trib1 down-regulates NF-IL6–dependent activation, HEK293 cells were transfected with an NF-IL6–dependent luciferase reporter plasmid together with NF-IL6 and various amounts of Trib1 expression vectors (Fig. 3 A). NF-IL6–mediated luciferase activity was diminished by co-expression of Trib1 in a dose-dependent manner. Moreover, RAW264.7 macrophage cells overexpressing Trib1 exhibited reduced expression of mPGES and 24p3 in response to LPS (Fig. S3 A, available at http://www.jem.org/cgi/content/full/jem.20070183/DC1). We next tested NF-IL6 DNA-binding activity by EMSA and observed less NF-IL6 DNA-binding activity in HEK293 cells coexpressing NF-IL6 and Trib1 than in ones transfected with the NF-IL6 vector alone (Fig. 3 B), presumably accounting for the down-regulation of the NF-IL6–dependent gene expression by Trib1. We then examined the effect of Trib1 on the amounts of NF-IL6 proteins by Western blotting. Although the diminution of NF-IL6 by Trib1 was marginal when excess amounts of NF-IL6 were expressed, we found that the transient expression of lower levels of NF-IL6, together with Trib1, resulted in a reduction of NF-IL6 in HEK293 cells (Fig. 3 C). Also, endogenous levels of NF-IL6 proteins in RAW264.7 cells overexpressing Trib1 were markedly less than those in control cells (Fig. 3 D). These results demonstrated that overproduction of Trib1 might negatively regulate NF-IL6 activity in vitro.

Up-regulation of NF-IL6 in Trib1-deficient cells

We next attempted to check the in vivo status of NF-IL6 in Trib1-deficient cells by comparing the NF-IL6 DNA-binding activity in Trib1-deficient macrophages with that in wild-type cells by EMSA. Although LPS-induced NF-κB–DNA complex formation in Trib1-deficient cells was similarly observed, Trib1-deficient cells exhibited elevated levels of C/EBP–DNA complex formation compared with wild-type cells (Fig. 4 A). We further examined whether the C/EBP–DNA complex in Trib1-deficient cells contained NF-IL6 by supershift assay. Addition of anti–NF-IL6 antibody into the C/EBP–DNA complex yielded more supershifted bands in Trib1-deficient cells than in wild-type cells (Fig. 4 B). In addition, the C/EBP–DNA complex was not shifted by the addition of anti-C/EBPδ (also known as NF-IL6β) antibody (Fig. S4 A, available at http://www.jem.org/cgi/content/full/jem.20070183/DC1), suggesting that NF-IL6 DNA-binding activity is augmented in Trib1-deficient cells. We then examined the amounts of NF-IL6 proteins by Western blotting (Fig. 4 C). Compared with wild-type cells, Trib1-deficient cells showed increased levels of NF-IL6 proteins. Finally, we examined NF-IL6 mRNA levels by Northern blotting and observed enhanced expression of NF-IL6 mRNA in Trib1-deficient cells (Fig. 4 D), which is consistent with the autocrine induction of NF-IL6 mRNA

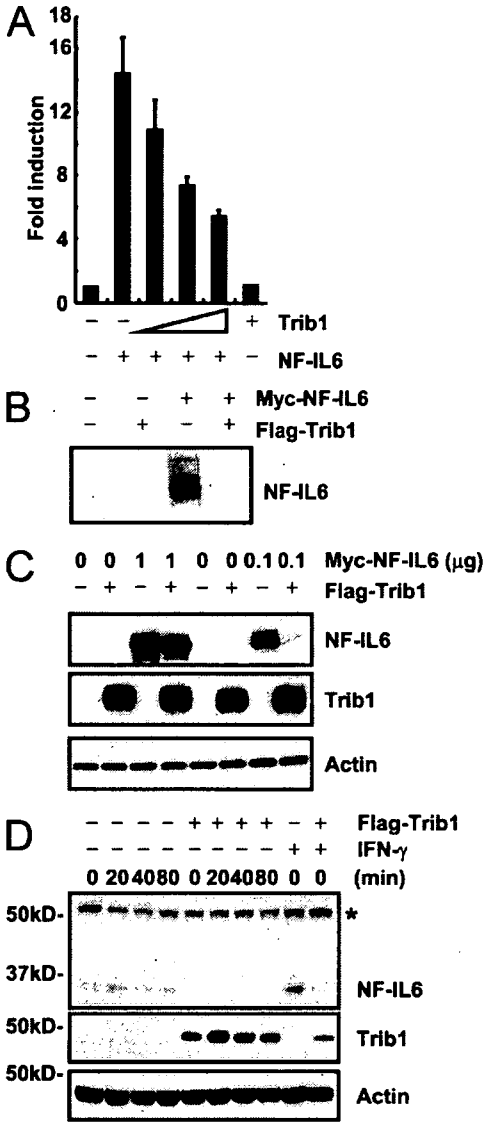

Figure 3. Inhibition of NF-IL6 activity by Trib1 overexpression. (A) HEK293 cells were transfected with an NF-IL6–dependent luciferase reporter together with either Trib1 and/or NF-IL6 expression plasmids. Luciferase activities were expressed as the fold increase over the background shown by lysates prepared from mock-transfected cells. Indicated values are means ± SD of triplicates. (B) HEK293 cells were transfected with 0.1 μg NF-IL6 expression vector together with 4 μg Trib1 expression plasmids. Nuclear extracts were prepared, and C/EBP DNA-binding activity was determined by EMSA using a probe containing the NF-IL6 binding sequence from the mouse 24p3 gene. (C) Lysates of HEK293 cells transiently cotransfected with 2 μg of Flag-tagged Trib1 alone or the indicated amounts of Myc-tagged NF-IL6 expression vectors were immunoblotted with anti-Myc or -Flag for detection of NF-IL6 or Trib1, respectively. (E) RAW 264.7 cells stably transfected with either an empty vector or Flag-Trib1 were stimulated with 10 ng/ml LPS for the indicated periods. The cell lysates were immunoblotted with the indicated antibodies. A protein that cross-reacts with the antibody is indicated (*). Data are representative of three (A and C) and two (B and D), separate experiments.

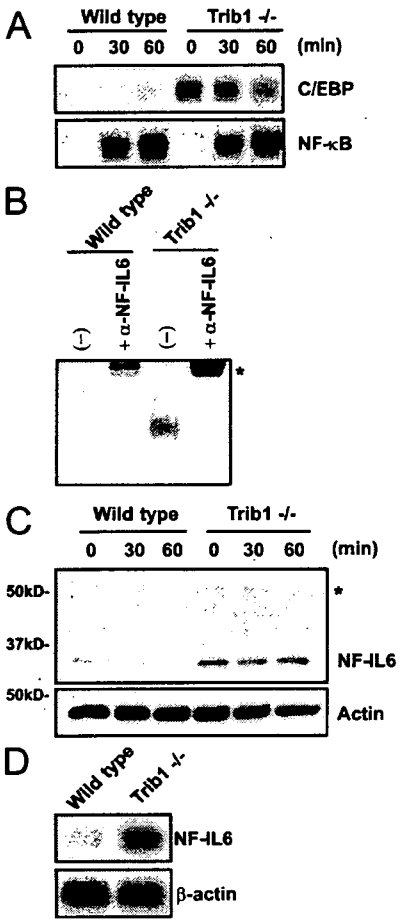

Figure 4. Up-regulation of NF-IL6 activity in Trib1-deficient cells. (A) Peritoneal macrophages from wild-type or Trib1-deficient mice were stimulated with 10 ng/ml LPS for the indicated periods. Nuclear extracts were prepared, and C/EBP DNA-binding activity was determined by EMSA using a C/EBP consensus probe. (B) Nuclear extracts of wild-type and Trib1-deficient unstimulated macrophages were preincubated with anti-NF-IL6, followed by EMSA to determine the C/EBP DNA-binding activity. Supershifted bands are indicated (*). (C) Peritoneal macrophages from wild-type or Trib1-deficient mice were stimulated with 10 ng/ml LPS for the indicated periods and lysed. The cell lysates were immunoblotted with the indicated antibodies. A protein that cross-reacts with the antibody is indicated (*). (D) Total RNA (10 μg) from unstimulated peritoneal macrophages from wild-type or NF-IL6-deficient mice was extracted and subjected to Northern blot analysis for expression of the indicated probes. Data are representative of two (A and B) and three (C and D) separate experiments.

in a previous study (15). Thus, Trib1 may negatively control amounts of NF-IL6 proteins, thereby affecting TLR-mediated NF-IL6–dependent gene induction.

DISCUSSION

In this study, we demonstrate by microarray analysis and biochemical studies that Trib1 is associated with NF-IL6 and negates NF-IL6–dependent gene expression by reducing the amounts of NF-IL6 proteins in the context of TLR-mediated responses. Especially regarding IL-12 p40, although the microarray data showed an almost twofold reduction of the mRNA in Trib1-deficient cells (Table S1), the production was three to four times lower than that in wild-type cells (Fig. 1 C), suggesting translational control of IL-12 p40 by Trib1 in addition to the transcriptional regulation. Moreover, the transcription of the IL-12 p40 gene itself may be affected by not only the amount of NF-IL6 proteins but also the phosphorylation or the isoforms such as liver-enriched activator protein and liver-enriched inhibitory protein (16–18). The molecular mechanisms of how Trib1 deficiency affects IL-12 p40 production on the transcriptional or translational levels through NF-IL6 regulation need to be carefully studied in the future.

The name Trib is originally derived from the *Drosophila* mutant strain *tribbles*, in which the *Drosophila* tribbles protein negatively regulates the level of *Drosophila* C/EBP *slbo* protein and C/EBP-dependent developmental responses such as border cell migration in larvae (19–22). It is also of interest that Trib1-deficient female mice and *Drosophila* in adulthood are both infertile (unpublished data) (18). In mammals, other Trib family members such as Trib2 and Trib3 have recently been shown to be involved in C/EBP-dependent responses (23, 24). Mice transferred with bone marrow cells, in which Trib2 is retrovirally overexpressed, display acute myelogenous leukemia–like disease with reduced activities and amounts of C/EBPα (23). In addition, ectopic expression of Trib3 inhibits C/EBP-homologous protein–induced ER stress–mediated apoptosis (24). Thus, the function of tribbles to inhibit C/EBP activities by controlling the amounts appears to be conserved throughout evolution.

Given the up-regulation of the mRNA in Trib1-deficient cells (Fig. 4 D), the reduction of NF-IL6 in Trib1-overexpressing cells (Fig. 3 C), the auto-regulation of NF-IL6 by itself (15), and the degradation of C/EBPα by Trib2 (23) and slbo by tribbles (22), the loss of Trib1 might primarily result in impaired degradation of NF-IL6 and, subsequently, in excessive accumulation of NF-IL6 via the autoregulation in Trib1-deficient cells.

In this study, we focused on the involvement of Trib1 in TLR-mediated NF-IL6–dependent gene expression. However, given that the levels of NF-IL6 proteins were increased in Trib1-deficient cells, it is reasonable to propose that other non–TLR-related NF-IL6–dependent responses might be enhanced in Trib1-deficient mice. Moreover, Trib3 is also shown to be involved in insulin-mediated Akt/PKB activation in the liver by mechanisms apparently unrelated to C/EBP, suggesting that Trib family members possibly function in a C/EBP-independent fashion (25–27). Future studies using mice lacking other Trib family members, as well as Trib1, may help to unravel the nature of mammalian tribbles in wider points of view.

MATERIALS AND METHODS

Generation of Trib1-deficient mice. A genomic DNA containing the *Trib1* gene was isolated from the 129/SV mouse genomic library and characterized by restriction enzyme mapping and sequencing analysis. The gene encoding mouse Trib1 consists of three exons. The targeting vector was constructed by replacing a 0.4-kb fragment encoding the second exon of the

Trib1 gene with a neomycin resistance gene cassette (*neo*) (Fig. S1 A). The targeting vector was transfected into embryonic stem cells (E14.1). G418 and gancyclovir doubly resistant colonies were selected and screened by PCR and Southern blot analysis (Fig. S1 B). Homologous recombinants were microinjected into C57BL/6 female mice, and heterozygous F1 progenies were intercrossed to obtain *Trib1*$^{+/-}$ mice. We interbred the heterozygous mice to produce offspring carrying a null mutation of the gene encoding Trib1. Trib1-deficient mice were born at the expected Mendelian ratio and showed a slight growth retardation with reduced body weight until 2–3 wk after birth (unpublished data). Trib1-deficient that mice survived for >6 wk were analyzed in this study. To confirm the disruption of the gene encoding Trib1, we analyzed total RNA from wild-type and Trib1-deficient peritoneal macrophages by Northern blotting and found no transcripts for Trib1 in Trib1-deficient cells (Fig. S1 C). All animal experiments were conducted with the approval of the Animal Research Committee of the Research Institute for Microbial Diseases at Osaka University.

Reagents, cells, and mice. LPS (a TLR4 ligand) from *Salmonella minnesota* Re 595 and anti-Flag were purchased from Sigma-Aldrich. BLP (TLR1/TLR2), MALP-2 (TLR2/TLR6), and CpG oligodeoxynucleotides (TLR9) were prepared as previously described (28). Antiphosphorylated extracellular signal-regulated kinase, Jnk, and p38 antibodies were purchased from Cell Signaling. Anti–NF-IL6 (C/EBPβ), C/EBPδ, actin, IκBα, and Myc-probe were obtained from Santa Cruz Biotechnology, Inc. NF-IL6–deficient mice were as previously described (29). Epitope-tagged Trib1 fragments were generated by PCR using cDNA from LPS-stimulated mouse peritoneal macrophages as the template and cloned into pcDNA3 expression vectors, according to the manufacturer's instructions (Invitrogen).

Measurement of proinflammatory cytokine concentrations. Peritoneal macrophages were collected from peritoneal cavities 96 h after thioglycollate injection and cultured in 96-well plates (10^5 cells per well) with the indicated concentrations of the indicated ligands for 24 h, as shown in the figures. Concentrations of TNF-α, IL-6, and IL-12 p40 in the culture supernatant were measured by ELISA, according to manufacturer's instructions (TNF-α and IL-12 p40, Genzyme; IL-6, R&D Systems).

Luciferase reporter assay. The NF-IL6–dependent reporter plasmids were constructed by inserting the promoter regions (−1200 to +53) of the mouse 24p3 gene amplified by PCR into the pGL3 reporter plasmid. The reporter plasmids were transiently cotransfected into HEK293 with the control *Renilla* luciferase expression vectors using a reagent (Lipofectamine 2000; Invitrogen). Luciferase activities of total cell lysates were measured using the Dual-Luciferase Reporter Assay System (Promega), as previously described (28).

Yeast two-hybrid analysis. Yeast two-hybrid screening was performed as described for the Matchmaker two-hybrid system 3 (CLONTECH Laboratories, Inc.). For construction of the bait plasmid, the full length of human Trib1 was cloned in frame into the GAL4 DNA-binding domain of pGBKT7. Yeast strain AH109 was transformed with the bait plasmid plus the human lung Matchmaker cDNA library. After screening of 10^6 clones, positive clones were picked, and the pACT2 library plasmids were recovered from individual clones and expanded in *Escherichia coli*. The insert cDNA was sequenced and characterized with the BLAST program (National Center for Biotechnology Information).

Microarray analysis. Peritoneal macrophages from wild-type or Trib1-deficient mice were left untreated or were treated for 4 h with 10 ng/ml LPS in the presence of 30 ng/ml IFN-γ. The cDNA was synthesized and hybridized to Murine Genome 430 2.0 microarray chips (Affymetrix), according to the manufacturer's instructions. Hybridized chips were stained and washed and were scanned with a scanner (GeneArray; Affymetrix). Microarray Suite software (version 5.0; Affymetrix) was used for data analysis. Microarray data have been deposited in the Gene Expression Omnibus under accession no. GSE8788.

Western blot analysis and immunoprecipitation. Peritoneal macrophages were stimulated with the indicated ligands for the indicated periods, as shown in the figures. The cells were lysed in a lysis buffer (1% Nonidet P-40, 150 mM NaCl, 20 mM Tris-Cl [pH 7.5], 5 mM EDTA) and a protease inhibitor cocktail (Roche). The cell lysates were separated by SDS-PAGE and transferred to polyvinylidene difluoride membranes. For immunoprecipitation, cell lysates were precleared with protein G–sepharose (GE Healthcare) for 2 h and incubated with protein G–sepharose containing 1 μg of the antibodies indicated in the figures for 12 h, with rotation at 4°C. The immunoprecipitants were washed four times with lysis buffer, eluted by boiling with Laemmli sample buffer, and subjected to Western blot analysis using the indicated antibodies, as previously described (28).

EMSA and supershift assay. 2×10^6 peritoneal macrophages were stimulated with the indicated stimulants for the indicated periods, as shown in the figures. 2×10^6 HEK293 cells were transfected with 0.1 μg Myc–NF-IL6 and/or 4 μg Flag-Trib1 expression vectors. Nuclear extracts were purified from cells and incubated with a probe containing a consensus C/EBP DNA-binding sequence (5′-TGCAGATTGCGCAATCTGCA–3′; Fig. 4, A and B) or mouse 24p3 NF-IL6 binding sequence (sense, 5′-CTTCCTGTTGCTCAACCTTGCA-3′;antisense,5′-TGCAAGGTTGAGCAACAGGAAG–3′; Fig. 3 B), electrophoresed, and visualized by autoradiography, as previously described (28, 30). When the supershift assay was performed, nuclear extracts were mixed with the supershift-grade antibodies indicated in the figures before the incubation with the probes for 1 h on ice.

Online supplemental material. Fig. S1 showed our strategy for the targeted disruption of the mouse *Trib1* gene. Fig. S2 showed the status of proinflammatory cytokine production in response to various TLR ligands and LPS-induced activation of MAP kinases and IκB degradation. Fig. S3 showed decreased expression of NF-IL6–dependent gene in Trib1-overexpressing cells. Fig. S4 showed that the C/EBP-DNA complex in Trib1-deficient cells contained NF-IL6, but not C/EBPδ. Table S1 provides a complete list of the LPS-inducible genes studied. Online supplemental material is available at http://www.jem.org/cgi/content/full/jem.20070183/DC1.

We thank M. Hashimoto for excellent secretarial assistance, and N. Okita, N. Iwami, N. Fukuda, and M. Morita for technical assistance.

This study was supported by the Special Coordination Funds, the Ministry of Education, Culture, Sports, Science and Technology, research fellowships from the Japan Society for the Promotion of Science for Young Scientists, the Uehara Memorial Foundation, the Naito Foundation, the Institute of Physical and Chemical Research Junior Research Associate program, and the National Institutes of Health (grant AI070167).

The authors have no conflicting financial interests.

Submitted: 24 January 2007
Accepted: 26 July 2007

REFERENCES

1. Akira, S., S. Uematsu, and O. Takeuchi. 2006. Pathogen recognition and innate immunity. *Cell.* 124:783–801.
2. Beutler, B. 2004. Inferences, questions and possibilities in Toll-like receptor signalling. *Nature.* 430:257–263.
3. Kopp, E., and R. Medzhitov. 2003. Recognition of microbial infection by Toll-like receptors. *Curr. Opin. Immunol.* 15:396–401.
4. Hayden, M.S., and S. Ghosh. 2004. Signaling to NF-κB. *Genes Dev.* 18:2195–2224.
5. Zhang, Y.L., and C. Dong. 2005. MAP kinases in immune responses. *Cell. Mol. Immunol.* 2:20–27.
6. Miggin, S.M., and L.A. O'Neill. 2006. New insights into the regulation of TLR signaling. *J. Leukoc. Biol.* 80:220–226.
7. Hegedus, Z., A. Czibula, and E. Kiss-Toth. 2007. Tribbles: A family of kinase-like proteins with potent signalling regulatory function. *Cell. Signal.* 19:238–250.
8. Kiss-Toth, E., S.M. Bagstaff, H.Y. Sung, V. Jozsa, C. Dempsey, J.C. Caunt, K.M. Oxley, D.H. Wyllie, T. Polgar, M. Harte et al. 2004.

Human tribbles, a protein family controlling mitogen-activated protein kinase cascades. *J. Biol. Chem.* 279:42703–42708.
9. Wilkin, F., N. Suarez-Huerta, B. Robaye, J. Peetermans, F. Libert, J.E. Dumont, and C. Maenhaut. 1997. Characterization of a phosphoprotein whose mRNA is regulated by the mitogenic pathways in dog thyroid cells *Eur. Eur. J. Biochem.* 248:660–668.
10. Mayumi-Matsuda, K., S. Kojima, H. Suzuki, and T. Sakata. 1999. Identification of a novel kinase-like gene induced during neuronal cell death. *Biochem. Biophys. Res. Commun.* 258:260–264.
11. Wu, M., L.G. Xu, Z. Zhai, and H.B. Shu. 2003. SINK is a p65-interacting negative regulator of NF-κB-dependent transcription. *J. Biol. Chem.* 278:27072–27079.
12. Kiss-Toth, E., D.H. Wyllie, K. Holland, L. Marsden, V. Jozsa, K.M. Oxley, T. Polgar, E.E. Qwarnstrom, and S.K. Dower. 2006. Functional mapping and identification of novel regulators for the Toll/Interleukin-1 signalling network by transcription expression cloning. *Cell. Signal.* 18:202–214.
13. Uematsu, S., M. Matsumoto, K. Takeda, and S. Akira. 2002. Lipopolysaccharide-dependent prostaglandin E(2) production is regulated by the glutathione-dependent prostaglandin E(2) synthase gene induced by the Toll-like receptor 4/MyD88/NF-IL6 pathway. *J. Immunol.* 168:5811–5816.
14. Gorgoni, B., D. Maritano, P. Marthyn, M. Righi, and V. Poli. 2002. C/EBPβ gene inactivation causes both impaired and enhanced gene expression and inverse regulation of IL-12 p40 and p35 mRNAs in macrophages. *J. Immunol.* 168:4055–4062.
15. Ramji, D.P., and P. Foka. 2002. CCAAT/enhancer-binding proteins: structure, function and regulation. *Biochem. J.* 365:561–575.
16. Plevy, S.E., J.H. Gemberling, S. Hsu, A.J. Dorner, and S.T. Smale. 1997. Multiple control elements mediate activation of the murine and human interleukin 12 p40 promoters: evidence of functional synergy between C/EBP and Rel proteins. *Mol. Cell. Biol.* 17:4572–4588.
17. Zhu, C., K. Gagnidze, J.H. Gemberling, and S.E. Plevy. 2001. Characterization of an activation protein-1-binding site in the murine interleukin-12 p40 promoter. Demonstration of novel functional elements by a reductionist approach. *J. Biol. Chem.* 276:18519–18528.
18. Bradley, M.N., L. Zhou, and S.T. Smale. 2003. C/EBPβ regulation in lipopolysaccharide-stimulated macrophages. *Mol. Cell. Biol.* 23:4841–4858.
19. Seher, T.C., and M. Leptin. 2000. Tribbles, a cell-cycle brake that coordinates proliferation and morphogenesis during *Drosophila* gastrulation. *Curr. Biol.* 10:623–629.
20. Mata, J., S. Curado, A. Ephrussi, and P. Rorth. 2000. Tribbles coordinates mitosis and morphogenesis in *Drosophila* by regulating string/CDC25 proteolysis. *Cell.* 101:511–522.
21. Grosshans, J., and E. Wieschaus. 2000. A genetic link between morphogenesis and cell division during formation of the ventral furrow in *Drosophila*. *Cell.* 101:523–531.
22. Rorth, P., K. Szabo, and G. Texido. 2000. The level of C/EBP protein is critical for cell migration during *Drosophila* oogenesis and is tightly controlled by regulated degradation. *Mol. Cell.* 6:23–30.
23. Keeshan, K., Y. He, B.J. Wouters, O. Shestova, L. Xu, H. Sai, C.G. Rodriguez, I. Maillard, J.W. Tobias, P. Valk, et al. 2006. Tribbles homolog 2 inactivates C/EBPα and causes acute myelogenous leukemia. *Cancer Cell.* 10:401–411.
24. Ohoka, N., S. Yoshii, T. Hattori, K. Onozaki, and H. Hayashi. 2005. TRB3, a novel ER stress-inducible gene, is induced via ATF4-CHOP pathway and is involved in cell death. *EMBO J.* 24:1243–1255.
25. Du, K., S. Herzig, R.N. Kulkarni, and M. Montminy. 2003. TRB3: a tribbles homolog that inhibits Akt/PKB activation by insulin in liver. *Science.* 300:1574–1577.
26. Koo, S.H., H. Satoh, S. Herzig, C.H. Lee, S. Hedrick, R. Kulkarni, R.M. Evans, J. Olefsky, and M. Montminy. 2004. PGC-1 promotes insulin resistance in liver through PPAR-alpha-dependent induction of TRB-3. *Nat. Med.* 10:530–534.
27. Qi, L., J.E. Heredia, J.Y. Altarejos, R. Screaton, N. Goebel, S. Niessen, I.X. Macleod, C.W. Liew, R.N. Kulkarni, J. Bain, et al. 2006. TRB3 links the E3 ubiquitin ligase COP1 to lipid metabolism. *Science.* 312:1763–1766.
28. Yamamoto, M., T. Okamoto, K. Takeda, S. Sato, H. Sanjo, S. Uematsu, T. Saitoh, N. Yamamoto, H. Sakurai, K.J. Ishii, et al. 2006. Key function for the Ubc13 E2 ubiquitin-conjugating enzyme in immune receptor signaling. *Nat. Immunol.* 7:962–970.
29. Tanaka, T., S. Akira, K. Yoshida, M. Umemoto, Y. Yoneda, N. Shirafuji, H. Fujiwara, S. Suematsu, N. Yoshida, and T. Kishimoto. 1995. Targeted disruption of the NF-IL6 gene discloses its essential role in bacteria killing and tumor cytotoxicity by macrophages. *Cell.* 80:353–361.
30. Shen, F., Z. Hu, J. Goswami, and S.L. Gaffen. 2006. Identification of common transcriptional regulatory elements in interleukin-17 target genes. *J. Biol. Chem.* 281:24138–24148.

Usefulness of Quantitative Real-time PCR Assay for Early Detection of Cytomegalovirus Infection in Patients with Ulcerative Colitis Refractory to Immunosuppressive Therapies

Takuya Yoshino, MD, Hiroshi Nakase, MD, PhD,* Satoru Ueno, MD,* Norimitsu Uza, MD,* Satoko Inoue, MD,* Sakae Mikami, MD,* Minoru Matsuura, MD, PhD,* Katsuyuki Ohmori, MD, PhD,† Takaki Sakurai, MD, PhD,‡ Satoshi Nagayama, MD, PhD,§ Suguru Hasegawa, MD, PhD,§ Yoshiharu Sakai, MD, PhD,§ and Tsutomu Chiba, MD, PhD**

Background: Studies suggest that cytomegalovirus (CMV) infection exacerbates ulcerative colitis (UC) refractory to immunosuppressive therapies. Early and accurate diagnosis of CMV infection is important for the treatment of UC. We evaluated the usefulness of quantitative real-time polymerase chain reaction (PCR) for detecting CMV infection in inflamed colonic mucosa of patients with UC refractory to immunosuppressive therapies.

Methods: From 2003 to 2006, 30 patients (mean age: 41 ± 18 years; 14 men, 16 women) with UC refractory to immunosuppressive therapies were enrolled in the study. We evaluated CMV infection by CMV antigenemia, histologic examination, and quantitative real-time PCR for CMV using colonic mucosa and investigated the clinical outcomes of antiviral therapy.

Results: CMV-DNA was detected only in the inflamed colonic mucosa in 17 (56.7%) of 30 patients. Of the 17 CMV-DNA-positive patients, 4 were positive for CMV antigenemia or inclusion bodies on histologic examination; of the 13 CMV-DNA-negative patients none was positive for CMV antigenemia or inclusion bodies. Of the 17 CMV-DNA-positive patients, 12 (70.6%) were treated with ganciclovir for 2 weeks and 10 patients went into remission. Two other patients required colectomy after antiviral therapy. In contrast, of the 13 CMV-DNA-negative patients 12 (92.3%) achieved remission after intensifying their immunosuppressive therapies.

Conclusions: Quantitative real-time PCR assay for detecting CMV-DNA is useful for early, accurate diagnosis of CMV infection in patients with UC refractory to immunosuppressive therapies, enabling prompt and appropriate treatment.

(Inflamm Bowel Dis 2007;13:1516–1521)

Key Words: ulcerative colitis, cytomegalovirus, real-time PCR

Cytomegalovirus (CMV) infection is an important exacerbating factor in patients with ulcerative colitis (UC).[1–3] Because CMV infection occurs often in immunocompromised hosts,[4] CMV infection in patients with UC refractory to immunosuppressive therapies must always be considered a possibility. If CMV infection is not recognized at an early stage, appropriate treatment is not promptly initiated and the prognosis of patients with UC complicated by CMV infection is generally poor.[5,6] Thus, an accurate and rapid diagnosis of CMV infection is critical in UC patients refractory to immunosuppressive therapies.

Several modalities are currently used for detecting CMV infection.[7–9] For diagnosis of CMV infection in the gastrointestinal tract, combined CMV antigenemia assay and detection of CMV inclusion bodies in biopsy specimens from the gastrointestinal mucosa by either hematoxylin and eosin (H&E) staining or immunohistochemistry (IHC) using anti-CMV monoclonal antibodies has been proposed.[1] It is often difficult, however, to accurately diagnose CMV infection in patients with UC,[10] even when using this combined diagnostic method. Several recent studies indicate that the real-time polymerase chain reaction (PCR) assay allows for sensitive and rapid detection of CMV-DNA in clinical samples, and is more useful and beneficial for diagnosing CMV infection than CMV antigenemia assay or histologic examination.[11,12]

From the *Department of Gastroenterology & Hepatology, Graduate School of Medicine, Kyoto University, †Department of Clinical Laboratory, Kyoto University Hospital, ‡Laboratory of Diagnostic Pathology, Kyoto University Hospital, §Department of Surgery, Kyoto University Hospital, Kyoto, Japan.

Supported by a Grant-in-Aid for Scientific Research (C) from the Ministry of Culture and Science of Japan to Hisroshi Nakase (grant 18590677), and Grants-in-aid for Scientific Research (16017240, 16017249,17013051, 17659212, and 18012029) from the Ministry of Education, Culture, Sports, Science and Technology of Japan, Grant-in-aid for Scientific Research (15209024 and 18209027) from JSPS, and Grant-in-Aid for Research on Measures for Intractable Diseases, and Research on Advanced Medical Technology (nano005) from the Ministry of Health, Labor, and Welfare, Japan (to T.C.).

Reprints: Hiroshi Nakase, MD, PhD, Department of Gastroenterology & Hepatology, Graduate School of Medicine, Kyoto University, 54 Kawahara-cho, Shogoin, Sakyo-ku, Kyoto, 606-8507, Japan. (e-mail: hiropy-n@kuhp.kyoto-u.ac.jp).

DOI 10.1002/ibd.20253

Published online 7 September 2007 in Wiley InterScience (www.interscience.wiley.com).

TABLE 1. Endoscopic Index of Rachmilewitz[16]

Items	Scores			
	0	1	2	4
1. Granulation scattering reflected light	No	—	Yes	—
2. Vascular pattern	Normal	Faded/disturbed	Completely absent	—
3. Vulnerability of mucosal	None	—	Slightly increased (contact bleeding)	Greatly increased (spontaneous bleeding)
4. Mucosal damage (mucus, exudates, erosions, ulcer)	None	—	Slight	Pronounced

Total score is sum of the item scores.

A conventional PCR assay, however, might also detect a latent CMV infection that has nothing to do with the deterioration of UC.[11] We recently applied quantitative real-time PCR for detecting CMV in patients with UC refractory to immunosuppressive therapies and found that the CMV-DNA copy number is higher in inflamed colonic mucosa than in noninflamed mucosa in these patients, suggesting the usefulness of this method to accurately diagnose active CMV infection.[13,14]

In the present study we further examined the usefulness of the quantitative real-time PCR assay using colonic mucosa for diagnosing active CMV infection in patients with UC. An accurate diagnosis of CMV infection might enable a more effective treatment for patients with UC refractory to immunosuppressive therapies.

MATERIALS AND METHODS

Patients

Among 93 patients with UC (55 men, 38 women) that visited Kyoto University Hospital from October 2003 to October 2006, 30 patients with UC refractory to immunosuppressive therapies, including steroids and immunomodulators, were studied retrospectively. The diagnosis of UC was based on clinical, endoscopic, radiologic, and histologic parameters. Fecal bacterial culture yielded no specific pathogens in any of the patients. All patients had been treated with immunosuppressive therapies, and had active UC defined as moderate to severe using the disease activity index (DAI) criteria,[15] with a score greater than 6 points.

Assessment of Endoscopic Severity

Endoscopic severity of UC was assessed using the DAI score,[15] Matts grade,[16] and the Endoscopic index of Rachmilewitz.[17] Endoscopic findings were scored from 0 to 3 according to DAI scores as: normal = 0, mild friability = 1, moderate friability = 2, and spontaneous bleeding = 3, and also scored from 1 to 4 according to Matts grade as: normal = 1, mild granularity and edema = 2, marked granularity and edema, and spontaneous bleeding = 3, severe ulceration = 4. The endoscopic index of Rachmilewitz is shown in Table 1.

Histopathology

Colonic biopsies were fixed in formalin, embedded in paraffin, stained with H&E, and IHC was performed using anti-CMV monoclonal antibodies (Dako Cytomation, Kyoto, Japan).[13] These sections were evaluated for characteristic cytomegalic cells and "owl's-eye" nuclear inclusion bodies.

CMV Antigenemia

The antigenemia assay was performed using a monoclonal antibody (C7HRP or C10C11) against a CMV structural protein of the 65 kDa lower-matrix phosphoprotein (pp65).[7,8]

Quantitative Real-time PCR

DNA for real-time PCR assay was extracted from the colonic tissues obtained from patients at endoscopic examination using QIAamp DNA Blood Mini Kit (Qiagen, Tokyo, Japan) according to the manufacturer's instructions. The assay was performed using an ABI Prism 7700 Sequence Detector System (Perkin Elmer Applied Biosystems, Foster City, CA) as described previously.[18] The oligonucleotide primers used for CMV-DNA amplification were constructed to detect the immediate early gene. The upstream primer was 5′-GACTAGTGTGATGCTGGCCAAG-3′ and the downstream primer was 5′-GCTACAATAGCCTCTTCCTCATCTG-3′. The 6-carboxyfluorescein-labeled probe was 5′-AGCCTGAGGTTATCAGTGTAATGAAGCGCC-3′. The PCR conditions were incubation at 95°C for 10 minutes, 50 cycles of 95°C for 15 seconds, followed by incubation at 62°C for 1 minute. Cases in which the CMV-DNA copy number was over 10 copies/μg DNA were defined as positive for CMV infection.

Diagnosis of CMV Infection

Cases that were detected as CMV infection by at least one of these methods (histopathology, CMV antigenemia, and quan-